MECHANICAL PROPERTIES CHARACTERIZATION OF ADVANCED COMPOSITE MATERIALS, A REVIEW

Peter Rolando Alvarado Prieto, M.Eng.

Lead Engineer
Colombian Air Force

Science and Air Power Collection No 8

Colombian Air Force Graduate School

MECHANICAL PROPERTIES CHARACTERIZATION OF ADVANCED COMPOSITE MATERIALS, A REVIEW

First Edition

Peter Rolando Alvarado Prieto, M.Eng.

Lead Engineer
Colombian Air Force

Science and Air Power Collection Nº 8

Bogota D.C., November 2014

Library of Graduate School of the Colombian Air Force Cataloging-in-Publication Data

Alvarado Prieto, Peter Rolando

Mechanical Properties Characterization of Advanced Composite Materials: a Review / Lieutenant Peter Rolando Alvarado Prieto. -- Bogota: Graduate School of the Colombian Air Force, 2014.

150p. : il. 24cm. – (Science and Air Power; No.8)

Includes bibliography for each chapter.

ISBN: XX-XXX-XXX

1. Composite materials--Industrial applications 2. Calima T-90 (Training plane) – Design and construction – Colombia 3. Aircraft industry—Military aspects – Colombia 4. Materiales Compuestos – Manufactura [Spanish] 5. Industria Aeronáutica – Aspectos Militares – Colombia [Spanish]

I. Colombia. Fuerza Aérea Colombiana

TA418.9.C6A48 2014

620.118 A472m--dc23

November 28, 2014

Alvarado, P. (2014). *Mechanical Properties Characterization of Advanced Composite Materials: a Review.* First edition. Science and Air Power Collection No. 8. Bogota, Colombia: Graduate School of the Colombian Air Force

Research book
First Edition: Bogota November de 2014
Science and Air Power Collection No. 8
ISBN:
Number of copies: 500
Printed and made in Colombia

Style checking: Strategy Ltda.
Design and printing: Strategy Ltda.

Carrera 11 No. 102-50 Building ESDEGUE, office 411
Bogota, Colombia. A.A. 110111
Tel: (0571) 6378927 - (0571) 6206518 Ext. 1700
Please forward any suggestions or comments to: cienciaypoderaereo@epfac.edu.co / peteralvaradoprieto@gmail.com
www.epfac.edu.co

About the work

The Colombian Air Force Graduate School presents as part of the Science and Air Power Collection, in its Vol. Nº8, the work entitled "Mechanical Properties Characterization of Advanced Composite Materials" by Lieutenant Peter Rolando Alvarado Prieto, as a result of research carried on at Purdue University and in the Colombian Air Force.

This book is intended to improve the technical understanding and practical knowledge about composite materials characterization of practicing engineers, researchers and students. Particularly for the Colombian Air Force, it will be used as a guide during the T-90 aircraft certification program where the author is participating. May it also contribute for new materials development and its use in future aircraft designs in Colombia.

Should this be the opportunity to praise the author's commitment and scientific contribution; during his career at the Air Force he has always look forward to work in research projects and to put all his efforts for a better future and development of his nation. On the other hand, having allowed us to publish his work in English language is setting a reference point for other researchers, who should be encouraged to write in a foreign language.

This work would not have been possible without the acceptance of the scientific community, represented by professor Miguel Angel Hidalgo Salazar, MSc in Mechanical Engineering (Col-Uniandes), PhD in Engineering - Materials, Polymers, and Composites (Col-Univalle); and professor Edgar Alejandro Marañon Leon, MSc in Mechanical Engineering (Col-Unian-

des), PhD in Damage Characterization of Composite Materials (UK- Loughbrorough). Special thanks for their significant contribution that allowed us to successfully culminate this project.

Finally, I am sure that this publication is of great importance and will be used as a reference for the development of science, technology, and innovation in our country.

Colonel
Gerber Johan Alzate Gutiérrez
Director of the Colombian Air Force Graduate School

Acknowledgements

This book is a collaborative effort. It wouldn´t have been possible without the support from my family, the Air Force´s Graduate School staff, people from MSE 597 of spring 2011, and last but definitely not the least, Professors Byron Pipes and C.T. Sun to whom I owe the knowledge acquired in this matter.

Especial thanks to my wife, Ekaterina, who helped me and supported me during the writing process, brought me tasty food, controlled my writing production in the best possible way, gave me tenderness when I needed the most, and worked by my side at nights.

To my mother, Marlen, and my father, Pedro, from whom I am always thank full. I am who I am because you.

Many thanks to Colonel Alzate, who made this to become a reality, to Mayor Jaramillo for his aid during the edition process, to Mayden for her constant advices and recommendations, and to Diana, Erika, Alicia, Martha, and Carly, for the nice time spend while writing at their office.

Dedication

I dedicate this book to my mother, Marlen, my father, Pedro, my sister, Katherine, my brother, Jhonattan, and Lupita.

Preface

This content is a compilation of lessons learnt and knowledge acquired during research and work done at Purdue University and as a lead engineer in the Colombian Air Force, on advanced composites materials and characterization. Each topic addressed in the development of this document, will allow the reader to understand the basic concept of this matter, and to identify the tools, analysis and equations needed to fabricate and characterize advanced composite materials. As a whole was designed to assist the development of the Colombian Aerospace Industry as a guide during the experimental characterization of the composites materials used in the Calima T-90 aircraft and to be a reference for future aircraft development projects led by the Colombian Air Force. However, its application can extend beyond the aerospace field, since composite materials are also used in other areas such as sportive equipment, automobiles, construction, and ballistic protection, among others.

Chapter 1 introduces the topic of advanced composites which defines the basic concept required to understand the main topic of the book. It shows how to fabricate a composite laminate by the hand lay-up method using *prepreg* and autoclave curing. At the end of this chapter it is expected that the reader, with the necessary tools, materials and equipment, can be able to fabricate a flat composite laminate. In Chapter 2 it is shown how to obtain properties of Lamina Tensile from a tension test. It is an introduction to the testing procedure using tensile testing machine, strain gages and data acquisition systems. Chapter 3 explains how the in plane shear properties of composites can be obtained by testing a +-45 specimen in tension. In Chapter 4, besides of explaining how to perform test in off axis specimens, introduces the reader to failure prediction approaches in composite materials. Chapter

5 tells about the material Flexural Test. Chapter 6, introduces a design feature behavior of composite materials regarding holes. It shows how the strength changes depending on the hole sizes, and also introduces failure prediction criteria. Chapter 7 and 8 are about the Lamina and Laminate Coefficient of Thermal Expansion respectively, and finally, Chapter 9 is about the Mode I Fracture testing, to see how a crack propagates through a lamina.

Peter Alvarado
Colombia
Nov, 2014

Contents

List of Tables

Table

List of Figures

Figure

Chapter 1

Fabrication of Composite Laminate by Hand Lay-Up

Chapter 1

Fabrication of Composite Laminate by Hand Lay-Up

A composite material is the result of combining two or more materials to achieve specific structural properties superior to the properties of the individual materials from which is constructed (Federal Aviation Administration, 2012). To differentiate from other composites such as concrete, fiber reinforced composites are usually called advanced composite materials ACM (Smallman & Bishop, 1999). They are conformed by high-performance resin systems and high-strength, high-stiffness fiber reinforcement, and are substantially superior to structural metals and alloys on an equal weight basis (Pilato & Michno, 1994). As a result, lately ACM are replacing metals in several applications, especially in the aerospace sector where strength to weight ratio plays a crucial factor. For instance, 50% of the weight for the Boeing 787 Dreamliner is ACM, a sharp increase from 12% for the Boeing 777, and similarly 52% for Airbus 350XWB, as well as about 47% for Bombardier C Series airplane (Zhang, Zhang, & Xupo, 2011). In Colombia, the Air Force has led the use of composite materials being part of helicopters structure, and lately with the fabrication of the composites trainer Calima T-90.

The most common ACM used in aviation are the Carbon Fiber Reinforced Polymers CFRP and the Glass Fiber Reinforced Polymer GFRP (Chung, 2010). These fibers come in two main presentations: One in which the fibers are dry and other in which the fibers have been impregnated with resin called *prepreg.* During the fabrication of ACM, dry fibers can be impregnated with resin manually or using resin transfer method RTM, or vacuum assisted resin transfer method VARTM. On the other hand, prepreg does not require further resin contend since it comes with a specific volume fraction; in other words,

it contains the required percentage of resin per volume, to provide the best outcome properties. Given this advantage of *prepreg* over dry fibers, usually primary aircraft structural ACM components are manufactured with prepreg (Erhard, 2006). It is sold in rolls by yards and should be store below freezing point to reduce the rate of cure and thus increase storage life.

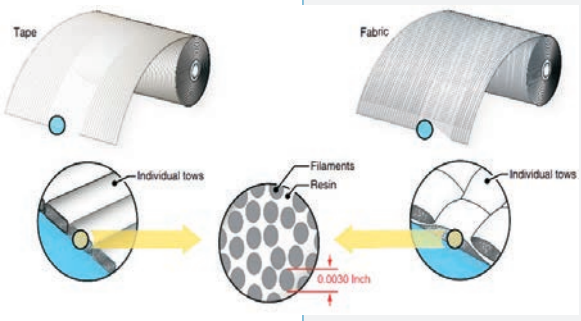

Figure 1. Unidirectional and bidirectional prepreg. *Source: Federal Aviation Administration (2012). Chapter 7. Advanced Composite Materials, pp.7-4. The Aviation Maintenance Technician Handbook—Airframe (FAA-H-8083-31).*

Prepreg may be unidirectional or bidirectional as shown in *Figure 1*. As its name indicates, in a unidirectional *prepreg* all fibers lay along one direction (longitudinal), usually called the $0°$ direction, while in a bidirectional prepreg certain fibers lay in the $0°$ and others perpendicular to them, in the transverse direction respectively, interlocking upon themselves. Unidirectional prepreg is called tape and bidirectional is called fabric.

Fiber orientation and stacking sequence

The outcome properties of the material depend on the plies and its orientation. In *Figure 2*, a warp clock is shown. It applies, both for unidirectional and bidirectional. It is used to identify fiber orientation. Moving in the clockwise direction, from 0 to 90 are the positive angles, and from 90 to 0 there are negative. From another perspective, moving in the counter clockwise direction represents the negative angles, and moving in the clockwise direction represents the positive angles, from 0 -90.

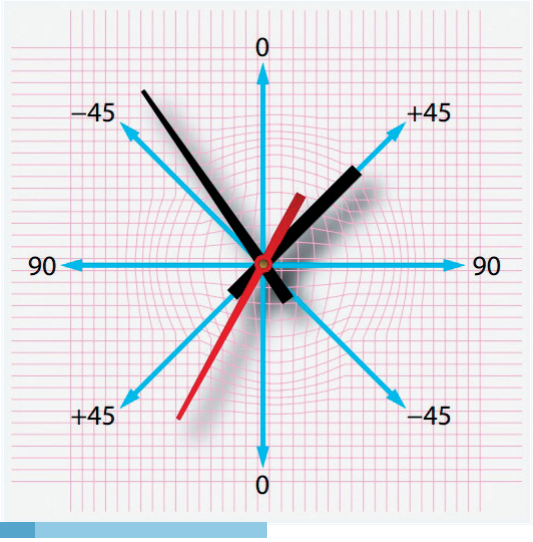

Figure 2. A warp clock. *Source: Federal Aviation Administration (2012). Chapter 7. Advanced Composite Materials, pp.7-3. The Aviation Maintenance Technician Handbook—Airframe (FAA-H-8083-31).*

Figure 3 shows an example of a stacking sequence $[0,90,\pm45]_s$. Note that the laminate contains 8 plies and that it symmetric on its middle plane; in other words, the four plies on the top are a mirror of the four plies on the bottom. If a laminate is not symmetric, while curing, the residual thermal stresses will cause deflections. Thus, if the desired outcome is a flat plate, it must be symmetric.

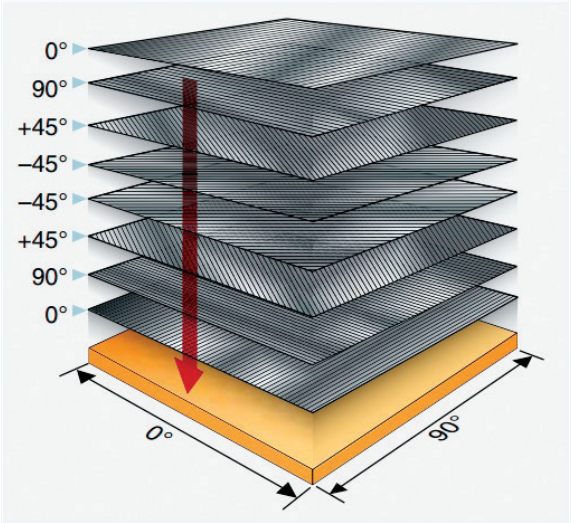

Figure 3. Example of stacking sequence. *Source: Federal Aviation Administration (2012). Chapter 7. Advanced Composite Materials, pp.7-3. The Aviation Maintenance Technician Handbook—Airframe (FAA-H-8083-31).*

Materials, tools and equipment

The following materials, tools and equipment are required for the fabrication of composite laminate by hand lay-up with *prepreg*:

- ***Materials***
  - Teflon films
  - Peel plies
  - Glass bleeders
  - Vent cloth
  - Sealant tape
  - Vacuum bag
  - Acetone
  - Release agent
  - Cork
  - Prepreg

- ***Tools***
  - Mold tool: It is what defines the final shape of the laminate. For a flat laminate, the mold tool can be a flat aluminum plate.
  - Vacuum valve
  - Knife
  - Scissors
  - Gloves
  - Personal protection items

- ***Equipment***
  - Autoclave

Procedure

The procedure for the fabrication of a composite laminate by hand lay - up with prepreg is the following:

1. Define the geometry of the laminate.
2. Define the material.
3. Define the stacking sequence.
4. Prepare materials, tools, and equipment required as mentioned in 0.
5. Take the *prepreg* out from the freezer and allow it to reach room temperature before using.
6. Cut *prepreg* according to the geometry and stac king sequence defined, see *Figure 4*.

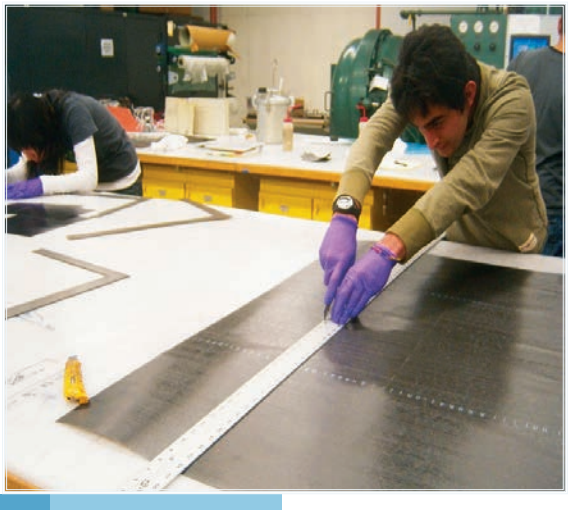

Figure 4. Prepreg cutting. *Source: MSE 597 report.*

7. Lay up the plies according to the stacking sequence, see *Figure 5*.
8. Clean the tool mold with acetone
9. Either apply release agent to the mold tool, or lay a Teflon film on the mold tool to be able to release the laminate after curing cycle, see *Figure 6*.
10. Lay a peel ply on the top of the Teflon film, if the desired bottom face of the laminate is a rough surface. This is optional and is usually done as a requirement step for surface bonding preparation because the peel ply generates

porosity in the outcome surface which at the end improves bonding strength (Flinn, 2014).

Figure 5. Lay-up process. *Source: MSE 597 report.*

11. Place the *prepreg* stack avoiding any wrinkle and leaving at least 50mm from the each edge.
12. Make a dam like structure surrounding the laminate to prevent from slicing.
13. Place a peel ply on the top of the *prepreg* stack.
14. Place a perforated Teflon film.
15. Place a bleeder sheet with the same dimensions of the laminate to absorb the excess of resin.
16. Place a perforated Teflon film.
17. Place a vent cloth usually called as breather on the top of the laminate with an extension for the vacuum valve, as shown in *Figure 7*. It is used to allow a uniform vacuum distribution, and is also a escaping route for volatiles.

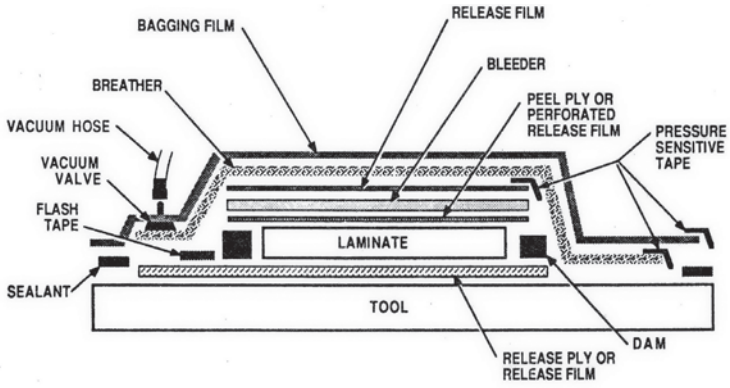

Figure 6. Vacuum bagging scheme. *Source: Carbonfiberguru (2010). Carbon Fiber Processing Part 2 of 12 – Vacuum Bagging.*

Figure 7. Bleeder and breather. *Source: MSE 597 report.*

18. Place the vacuum valve on the top of the breather avoiding any contact with the laminate as shown in *Figure 8*. For safety purposes, place Teflon under the breather, to avoid excess of resin going into the vacuum system.
19. Place sealant tape around the laid up structure on the mold tool.
20. Place the bagging film on the top of the whole arrangement and seal it against the sealant tape as shown in *Figure 6*.

Figure 8. Vacuum port on breather. *Source: MSE 597 report.*

21. Make a small cross cut on the bagging area located on the vacuum valve to install the vacuum hose.
22. Connect the vacuum hose to the vacuum valve as shown in Figure 9.
23. Put vacuum into the system and check for leaks. Maintain a vacuum of around 675mm of mercury for 20 min and check for leaks again. If any leak is found, verify sealing and change vacuum bag as required.

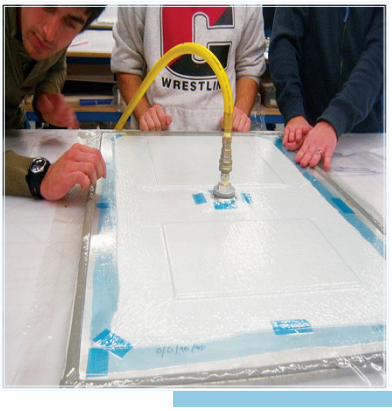

Figure 9. Vacuum bagging. *Source: MSE 597 report.*

24. Place the mold in the autoclave. An autoclave is a large pressure vessel with temperature and pressure control system, as the one shown in Figure 10.
25. Connect the autoclave vacuum hose to the stack vacuum valve.

Figure 10. Autoclave.
Source: Autoclave. Google images.

26. Properly close the autoclave doors.
27. Initiate curing cycle. Each *prepreg* or resin system comes with is specific curing cycle. However, a typical autoclave curing cycle is generally as follows *(see Figure 11)*: a first phase in which temperature is raised at a constant rate. Simultaneously, vacuum and pressure are applied. This removes any volatile that can be present in the laminates and eliminates any gap. The next phase is when temperature is held at $100°C$ approximately, for some hours to allow the resin to set in a uniform way among the fibers while chemical reaction is taking place. Then, it is heated up again and held at $180°C$ approximately. Finally, temperature is decreased at a constant rate during the cooling phase where pressure is kept. Several chemical reactions occur during the autoclave process. When the resin is heated up, its viscosity decreases and the pressure applied helps to remove any excess of resin. The resin passes through liquid, gel and vitrification stages.

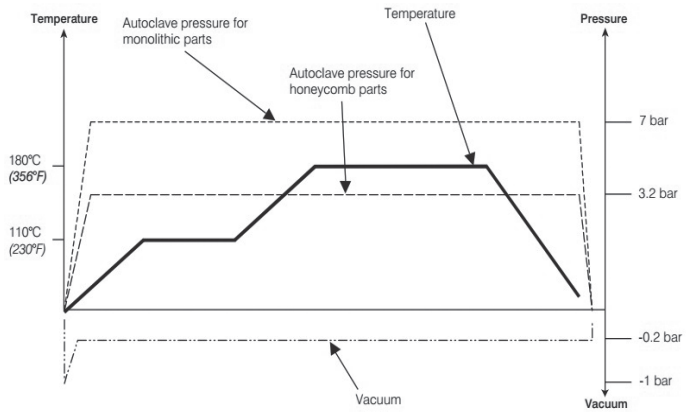

Figure 11. Typical prepreg curing cycle. *Source: HexPly 8552 Datasheet.*

28. Take the mold plate out of the autoclave and allow it to cool down.
29. Remove the vacuum bag and take out the laminate.
30. Inspect the laminate.

Conclusion

The fabrication of composites materials by lay-up process is a handicraft procedure in which the creation of new defects must be avoided at every time. The lay-up process has to be as clean as possible, and wrinkles in materials and layers must be avoided. Special care must be taken with the amount of time the *prepreg* has been exposed to room temperature, because it can complete the cure cycle before desired, and it would be no longer useful. It can be notice that the complexity of the process increase according with the desire geometry of the composites. For flat plate composite it is not as complex as for example with a geometry that involves sharp edges. However, the main principle remains the same. Another important factor is the orientation of the fiber in the laminate and its symmetry with respect to the middle plane. During the autoclave curing process, it goes into several temperature changes that cause

expansion and compression, which produce stresses. Those stresses produce different phenomena in the laminates regarding the symmetry and fiber orientation. The autoclave process involves heat transfer that should be taken into account to satisfy the temperature requirement in the curing process.

References

Chung, D. (2010). *Composite materials: Science and applications.* New York: Springer.

Erhard, G. (2006). *Designing with Plastics.* Munich: Hanser Publishers.

Federal Aviation Administration. (2012). *AMT Airframe Handbook Volume I (FAA-H-8083-31), Chapter 7 Advanced Composite Materials*. Retrieved from https://www.faa.gov/regulations_policies/handbooks_manuals/aircraft/amt_airframe_handbook

Flinn, B. D. (2014, 08 04). *Improving Adhesive Bonding of composites through surface characterization.* Retrieved from Advanced materials in transport aircraft structures 2007 meeting: https://depts.washington.edu/amtas/events/amtas_07fall/Phariss.pdf

Pilato, L., & Michno, M. J. (1994). *Advanced composite materials.* New York: Springer-Verlag.

Smallman, R. E., & Bishop, R. J. (1999). *Modern Physical Metallurgy and Materials Engineering.* Oxford: Butterworth-Heinemann.

Zhang, Z., Zhang, Y., & Xupo, O. (2011). Study on Key Certification Issues of Composite Airframe Structures for Commercial Transport Airplane. *Procedia Engineering,* Volume 17, 247-257.

Chapter 2

Lamina Tensile Properties

Chapter 2

Lamina Tensile Properties

A lamina or ply is the basic unit of a composite. It is because of its properties that one specific lamina is chosen in the design phase rather than another one. However, before starting the manufacturing process, as part of quality control procedures, test should be conducted to confirm material properties of a batch or roll of *prepreg* lay within the tolerance limits and datasheet specifications. The American Society for Testing and Materials (ASTM) is an organization that leads the development and delivery of international voluntary consensus standards and it has around 12000 standards used around the world in research and development, product testing and quality systems (ASTM, 2014). The ASTM 3039 is a Standard Test Method for Tensile Properties of Polymer Matrix of Composite Material (ASTM D 3039-14, 2014) that is used to determine the lamina tensile properties.

This chapter shows a procedure to obtain the tensile properties of a lamina using as an example a Carbon Fiber Reinforced Polymer (CFRP); The IM7-8552. It is a unidirectional carbon fiber *prepreg* from Hexcel[1] used in primary aerospace structures (Hexcel, 2014). The information that can be obtained about the material from a tensile test is: Tensile Strength, Modulus of Elasticity, and Poisson's ratio. Isotropic materials have the same mechanical properties in every direction, but on the other hand, anisotropic materials properties change with respect to the direction. So, in order to understand the mechanical behavior of a lamina it is necessary to know its

1 World leader provider of carbon fiber, reinforced fibers, pre-impregnated materials, honeycomb core, tooling materials and finish aircraft structures

properties about its principal axes. As it is shown in Figure 12, 1 is the axis parallel to the fibers which corresponds to the 0° direction, 2 is perpendicular to 1 corresponding to the 90° direction, and 3 is the normal direction to the plane created by 1 and 2.

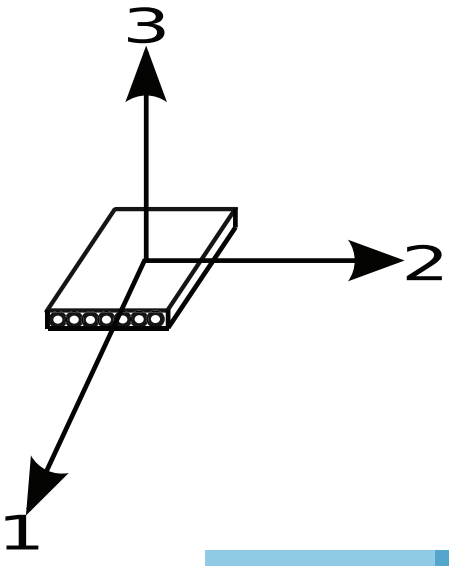

Figure 12. Lamina principal axes.
Author: Efunda.com (n.d.). Lamina Stress-Strain Relations for Principal Directions. Fibermax Composites.

Since lamina are also consider orthotropic due to a state of stress assumption of plain stress, then there is only need to know to its properties in the 0^0 and 90^0 directions. *Table 1* shows the properties of the IM7-8552 according to its datasheet (Hexcel, 2014). As would be expected both the tensile strength and the tensile modulus or modulus of elasticity in the 0^0 direction are higher than in the 90^0 direction. Thus, in order to obtain these properties from a lamina, two kinds of specimens need to be manufactured; one in the 0^0 direction and other in the 90^0 direction.

Table 1.

IM7-8552 Properties *(Hexcel, 2014)*

Test	Units	Temp °C (°F)	Condition	IM7
0° Tensile Strength	MPa (Ksi)	-55(-67) 25(77) 91(195)	Dry Dry Dry	2572 (373) 2724 (395) 2538 (368)
90° Tensile Strength	MPa (Ksi)	-55(-67) 25(77) 93(200)	Dry Dry Dry	174 (25.3) 111 (16.1) 92 (13.3)
0° Tensile Modulus	GPa (msi)	-55(-67) 25(77) 91(195)	Dry Dry Dry	163 (23.7) 164 (23.8) 163 (23.7)
90° Tensile Modulus	GPa (msi)	25(77) 93(200)	Dry Dry	12 (1.7) 10 (1.5)

Source: IM7-8552 Datasheet.

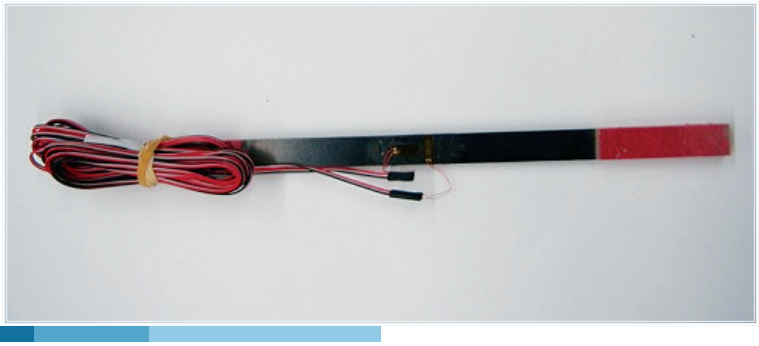

Figure 13. 0° **Specimen with strain gages.** *Source: Author.*

As mention above, in order to obtain the properties of a *prepreg* lamina, it is required to test specimens in the 0^0 direction and in the 90^0 direction. According to (ASTM D 3039-14, 2014) specimens should have a constant rectangular shape, thickness and width should be chosen to promote failure in the gage section, and the length should be large enough to minimize stress cause by minor grip eccentricities. In other words, there are not specific dimensions but there are some recommendations as shown in *Table 2*.

Table 2.

Recommended sample dimensions

Fiber orientation	Width, mm	Overall Length, mm	Thickness, mm	Tab Length, mm	Tab Thickness, mm
0° unidirectional	15	250	1	56	1,5
90° unidirectional	25	175	2	25	1,5
balanced and symmetric	25	250	2,5	emery cloth	--
random discontinuos	25	250	2,5	emery cloth	--

Source: Characterization of advanced composite materials.

It is recommended to manufacture panels and from them take the samples. The number of plies depends on the ply thickness of the lamina. For example, for a 0.127mm thick lamina, a 6 to 8 plies thick laminate will satisfy the recommended thickness for 0°, and a 16 to 24 plies thick laminate for the 90° (ASTM D 3039-14, 2014) recommends to test at least 5 samples but depending on the purpose of the results this amount may increase. So, panel(s) may be manufactured as shown in Chapter 1, and then cut according to the width recommended in *Table 2.*

Cutting composite panels is a delicate subject because damage can be induced and it could affect test result decreasing the tensile strength. They can be cut with a diamond saw by a specialized technician, with appropriate speed control and lubrication during the process. They can also be cut in a water jet, which generally provides cleaner cuts, though it is usually more expensive. It is important not to forget to account the

thickness of the cutting device for panel dimensions calculations. Anyway, samples should be visually inspected after being cut looking for edge delamination, or cracking.

End Tabs are used to avoid premature failure in the sample caused by the grips pressure. Glass fabric epoxy tabs are the most common nowadays, however before aluminum tabs were used as well. A structural adhesive such as Hysol EA 9394 should be used to bond the tabs to the specimens. An appropriate surface preparation should be done in the bonding area. A typical 0° carbon fiber specimen would be like the one shown in *Figure 13*, and a 90º specimen would be as the one shown in *Figure 14*.

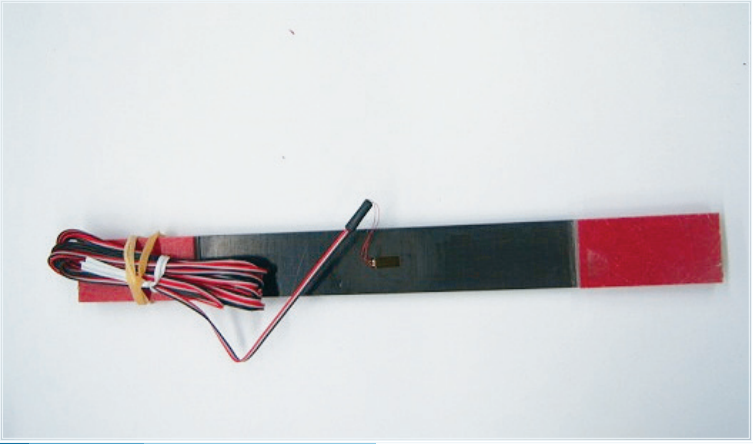

Figure 14. 90° Specimen with strain gage. *Source: Author.*

Materials, tools and equipment

The following materials, tools and equipment are required to obtain the lamina tensile properties:

- ***Materials***
  - » Specimens
  - » End Tabs
  - » Hysol EA 9394 or other structural adhesive
- ***Tools***
  - » Strain gages (2 x specimen)
  - » Personal protection items
  - » Caliper
- ***Equipment***
  - » Computer
  - » Data acquisition system
  - » Tensile testing machine
  - » Diamond saw or water jet

Procedure

The procedure to obtain the tensile properties of a lamina is as follows, according to ASTM 3039:

1. Manufacture panels according to Chapter 1.
2. Add the End Tabs
3. Cut panels using a diamond saw or water jet
4. Mark each specimen
5. Add strain gages to the sample

6. Measure and register each specimen thickness and width (3 measurements x specimen) as shown in *Figure 15*.

Figure 15. Specimen cross section measurement. *Source: MSE 597 report.*

7. Calculate cross sectional area
8. Connect a strain gage (already mounted to the sample) to the data acquisition system, see *Figure 16*.

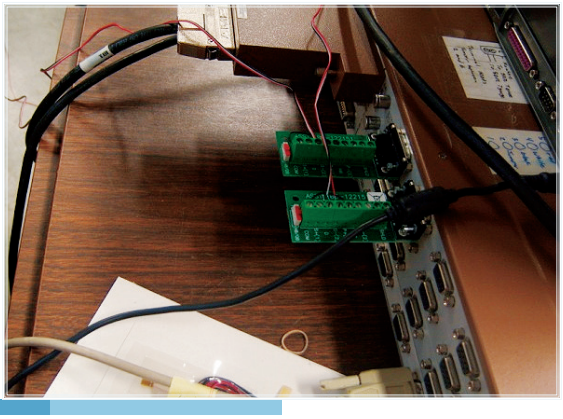

Figure 16. Acquisition system card. *Source: MSE 597 report.*

9. Prepare the tensile testing machine and the acquisition system
10. Clamp specimen in the tensile tester using the grips, *(see Figure 17)*.

Figure 17. Specimen clamping. *Source: MSE 597 report.*

11. Perform a tensile test at a rate of 2 mm/min while measuring the strain off the gage(s) as well as the load and displacement outputted from the tensile tester, *(see Figure 18)*.

Figure 18. Data acquisition software. *Source: MSE 597 report.*

12. Test to failure for 0o and 90o specimens

Failed specimens

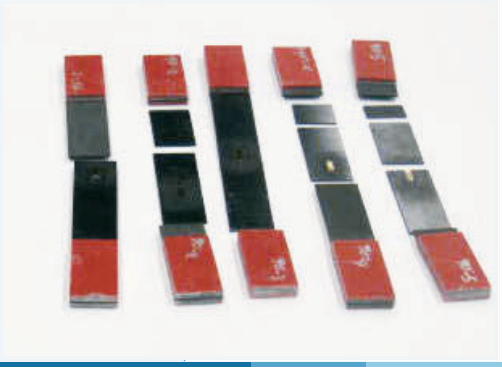

Figure 19. 90º specimen failed. *Source: MSE 597 report*

Figure 19 and *Figure 20* show a typical failure for the 0º and 90º specimens respectively. The 0º samples usually fail in an explosive way due to the high strength of the fibers in comparison with the matrix. That is way it is strongly recommended to use safety protection items at all time during the experi-

ments to avoid any accident. The 90º samples fail in the matrix and since there are not fibers in direction of the applied load, once the matrix has failed there is nothing standing the load. It is expected to have failure in the gage section, but as it can see on *Figure 19*, in reality some failures occur in other areas.

Figure 20. 0º Specimen failed. *Source: MSE 597 report.*

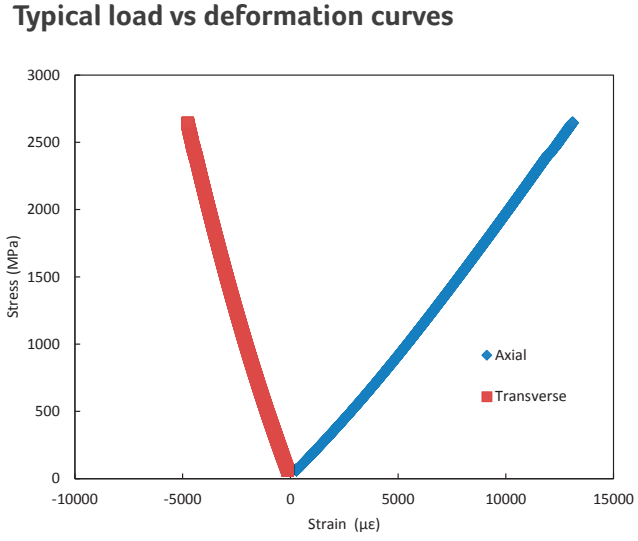

Figure 21. Stress vs deformation from a sample 0º sample. *Source: Author.*

A typical stress versus deformation plot from a lamina tensile test is shown in *Figure 21*. The blue line represents the strain captured by the strain gage in the axial direction and the orange line represents the strain captured in the transverse direction. Due to the lamina Poisson´s ratio the strain in the

transverse direction is negative which means that is being contracted. It can also be seen that the deformation in the axial direction is almost three times the deformation in the transverse direction.

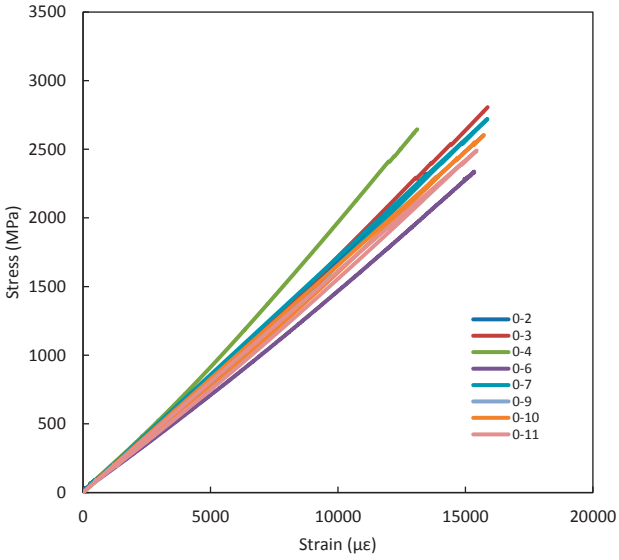

Figure 22.Typical stress vs deformation from 0º samples. *Source: Author.*

Furthermore, comparing the strength, which is the highest stress before failure, from the 0º and 90º specimens tests, as expected the 0º specimen have a higher strength than the 90º specimens, with approximately 2700MPa versus 75MPa respectively.

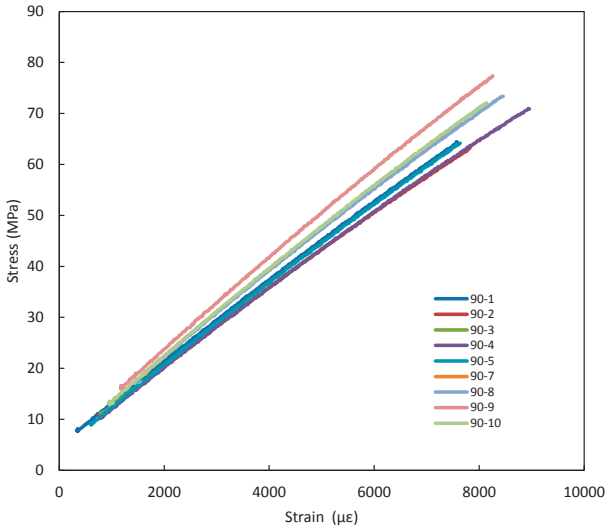

Figure 23. Typical stress vs deformation from 90º samples. *Source: Author.*

The expected behavior for the 0º and 90º specimens tensile test should be as shown on *Figure 22* and *Figure 23* respectively. The strain increases linearly as the load or stresses increases. However, it is important to be aware that the accuracy of the data provided by the strain gages could be affected by transverse deformation presented in the material, when it is axially loaded, due to the Poisson's ratio. The strain gages are design to capture the deformation in the longitudinal axes. However, this measure could be affected for the reasons stated previously. Because of that, transverse sensitiveness correction should be applied when: the stress field is not uniaxial, the gage is not parallel to the principal strain, or when the gage is mounted on a material different from the calibration material. For the effect of this example with IM7 8558 lamina, even though the gages are mounted on a material different from the material in which they were calibrate, which is usually steel, there is no need to have it into account, since in the 90º specimens the gages are parallel to the uniaxial stress, and in the 0º specimens the transverse gages sensitiveness correction can be neglected because of the small deformation presented in the longitudinal axes. It is usually better to have more spe-

cimens than the statistically required because there may be issues during the test with tabs, grip, strain gages, acquisition system, among others.

Data reduction

The raw data from the experiment is basically the load, which is given by the tensile testing machine, and the strains given by the strain gages in the data acquisition system. The axial stress is calculated for each sample dividing the load by the sample's average cross sectional area, which is calculated with the average thickness and width of each specimen.

Equation 1

$$\sigma = \frac{P}{A}$$

The four elastic constants E_1, E_2,, v_{12},and v_{21} are calculated according to ASTM D 3039. The tensile chord modulus of elasticity E was calculated by:

Equation 2

$$E = \frac{\Delta\sigma}{\Delta\varepsilon}$$

Where $\Delta\sigma$ is the difference in applied stress between two strain points used, and $\Delta\varepsilon$ is the difference between the two strain points used. Taking into account that the material is assume to be linearly elastic, and that data at the beginning of the test can be affected by setting up, the strain points used are typically $1000\,\mu\varepsilon$ and $3000\,\mu\varepsilon$.

So, E_1, that is the Modulus of elasticity in the fiber´s direction, would be calculated by *Equation 2* with $\Delta\sigma$ being the difference in stress from the 0º specimens and $\Delta\varepsilon$ being the difference in the axial stress from the 0º specimens as well. Similarly, E_2, the modulus of elasticity in the direction perpendicular to the fibers, would be calculated by *Equation 2*, with $\Delta\sigma$ being the difference in stress from the 90º specimens and $\Delta\varepsilon$ being the difference in the axial stress from the 90º specimens as well.

The Poisson's ratio ν_{12} is calculated by:

Equation 3

$$\nu_{12} = \frac{-\Delta\varepsilon_2}{\Delta\varepsilon_1}$$

Where $\Delta\varepsilon_2$ is the difference in transverse strain, $\Delta\varepsilon_1$ is the difference between two axial strain points. The Poisson's ratio ν_{21} is a dependent factor calculated by:

Equation 4

$$\nu_{21} = \frac{\nu_{12}E_2}{E_1}$$

The results from the tensile test used as an example during the chapter are shown in *Table 3*.

Table 3.

Tensile test example results

Property	Value
E_1	$156 \pm 11 GPa$
E_2	$8.46 \pm 0.51\ GPa$
X_1^T	$2.61 \pm 0.14\ GPa$
X_2^T	$0.066 \pm 0.01\ GPa$
v_{12}	0.34 ± 0.01
e_1^T	0.015
e_2^T	0.077

Source: Author.

References

ASTM D 3039-14. (2014). *Standard Test Method for Tensile Properties of Polymer Matrix Composite Materials.* West Conshohocken, PA: American Society for Testing and Materials.

ASTM. (2014, 08 05). Retrieved from American Society for Testing and Materials: http://www.astm.org/ABOUT/full_overview.html

Hexcel. (2014, 08 05). Retrieved from HexPly® 8552 Product Data: http://www.hexcel.com/Resources/DataSheets/Prepreg-Data-Sheets/8552_us.pdf

Chapter 3

In-Plane Shear Properties

In-Plane Shear Properties

When loading in tension on the axial axis a [±45] laminate coupon, shear response of a material can be analyzed. However, a state of biaxial stress is presented added to the shear stress (Sims, 1973). Moreover, in the laminate free edges there is presence of inter-laminar shear stress (Whitney J. M., 1973). For this reasons the shear strength can be underestimated. However, those effects are mitigated in the [±45] laminate due to the nonlinear response and low inter-laminar shear stress presented. In addition, comparing with other methods available to obtain the in plane shear properties of a polymer matrix composite material such as the Iosipescu Shear Test (Adams & Walrath, 1987) (Barnes, Kumosa, & Hull, 1987) or the v-notched rail shear test (Adams, Moriarty, Gallegos, & Adams, 2007), the [±45] tension shear test is easier to perform (R Wisnom, 1995). (ASTM D 3039-14, 2014), provides the recommendations for this test, which would be discussed during this chapter.

Chapter 3

Materials, tools and equipment

The following materials, tools and equipment are required to obtain the in plane shear properties of a polymer matrix composite material:

- ***Materials***
  - » Specimens
  - » End Tabs
  - » Hysol EA 9394 or other structural adhesive

- ***Tools***

  - » Strain gages (2 x specimen)
  - » Personal protection items
  - » Caliper

- ***Equipment***

  - » Computer
  - » Data acquisition system
  - » Tensile testing machine
  - » Diamond saw or water jet

Procedure

The procedure to obtain the in plane shear properties of a polymer matrix composite material is as follows:

1. Design [±45] tensile specimens in accordance with the ASTM standard D 3518.
2. Manufacture panels according to Chapter 1.
3. Add the End Tabs
4. Cut panels using a diamond saw or water jet
5. Mark each specimen
6. Add transverse and longitudinal strain gages to all the coupons.
7. Measure and register each specimen thickness and width (3 measurements x specimen)
8. Calculate cross sectional area
9. Connect a strain gage (already mounted to the sample) to the data acquisition system
10. Prepare a tensile testing machine displacement controlled and the data acquisition system.
11. Clamp specimen in the tensile tester using the grips, *(see Figure 17)*.

12. Test specimens at a rate of 2mm/min recording loads and displacements until failure.

Transverse sensitivity using a 2 gage rosette

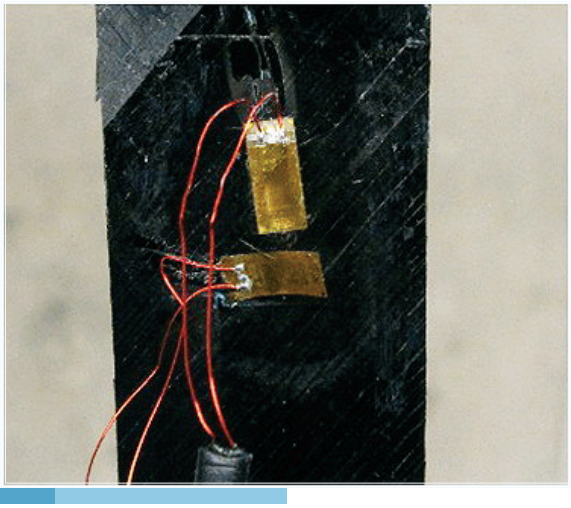

Figure 24. Strain gage mounted on specimen. *Source: Author.*

A 2 gage rosette is used to determine shear strain. However, the collected data should be corrected due the transverse sensitivity presented because the stress field is not uniaxial, the gage is not parallel to the principal strain in a uniaxial stress field, and the gage is mounted on material different from calibration material (TN-509, 2010). The corrected strains can be easily calculated by the following equations:

Equation 5

$$\varepsilon_x = \frac{(1-\nu_o K_t)(\hat{\varepsilon}_x - K_t \hat{\varepsilon}_y)}{1-K_t^{\,2}}$$

Equation 6

$$\varepsilon_y = \frac{(1-\nu_o K_t)(\hat{\varepsilon}_y - K_t \hat{\varepsilon}_x)}{1-K_t^{\,2}}$$

Where ε_x is the corrected strain in the x direction, ε_y is the corrected strain in the y direction, K_t is the transverse sensitivity coefficient, $\hat{\varepsilon}_x$ is the indicated strain in the x direction, $\hat{\varepsilon}_y$ is the indicated strain in the y direction, and ν_o is the Poisson's ratio for the calibration material, usually 0.285 (steel).

Data Reduction

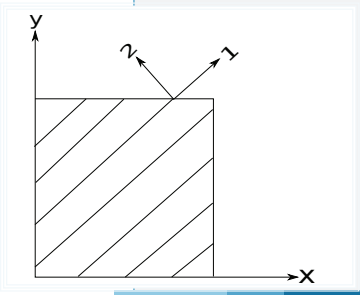

Figure 25. ±45 Specimen Coordinate System. *Author: Center for Composite Materials. (2004). Classical Lamination Theory. University of Delaware. On line http://www.ccm.udel.edu/Tech/CMAP/Manual_LaminateTheory.htm*

Figure 25 shows the coordinate system for a ±45 specimen. As explained in chapter 3, the 1 axis is parallel to the lamina fiber direction and the 2 axis is perpendicular to it. For a 0° lamina the 1 and the x axis are in the same direction, so the fiber and specimen coordinate system lay in the same directions. This is not the case for a 45° lamina where the specimen coordinate system is at 45° from the fiber coordinate system.

By the use of the coordinate transformation matrix, the state of the stresses and the strain with respect to the fibers main axis are calculated by *Equation 7* and *Equation 8*:

Equation 7

$$\begin{pmatrix} \sigma_1 \\ \sigma_2 \\ \tau_{12} \end{pmatrix} = \begin{pmatrix} m^2 & n^2 & 2mn \\ n^2 & m^2 & -2mn \\ -mn & mn & m^2-n^2 \end{pmatrix} \begin{pmatrix} \sigma_x \\ \sigma_y \\ \tau_{xy} \end{pmatrix}$$

Equation 8

$$\begin{pmatrix} \varepsilon \\ \varepsilon \\ {}_{12} \end{pmatrix} = \begin{pmatrix} m^2 & n^2 & mn \\ n^2 & m^2 & -mn \\ -mn & mn & m^2 - n^2 \end{pmatrix} \begin{pmatrix} \varepsilon \\ \varepsilon \\ {}_{xy} \end{pmatrix}$$

Where $m = \cos\theta$, and $n = \sin\theta$.

In a ±45 specimen tension test, the specimen is loaded in the x direction and so $\sigma_y = 0$ and $\theta = 45°$, substituting in the above equations the shear stress and strain in the fibers coordinate system are expressed by *Equation 9* and *Equation 10* respectively.

Equation 9

$$\tau_{12} = \frac{\sigma_x}{2}$$

Equation 10

$$\gamma_{12} = \varepsilon_x - \varepsilon_y$$

The engineering stress σ_x is calculated by *Equation 11*, where P_X is the tension load, w is the specimen width and t the specimen thickness.

Equation 11

$$\sigma_x = \frac{P_x}{wt}$$

The in-plane shear modulus can be calculated by two ways with the available data collected from the test. The first method is by calculating the slope of the shear stress shear versus strain curve. The second method is by using the relation of the

in-plane shear modulus with the poison's ratio and the elastic modulus for a rotation of 45°, as shown in *Equation 12*

Equation 12

$$G_{12} = \frac{E_x}{2(1+v_{xy})}$$

v_{xy} is calculated as $v_{xy} = E_x / E'_x$ where E_x is the slope of the tensile stress versus longitudinal strain curve, and E'_x is the slope of the longitudinal stress versus the transverse strain curve. Slopes are calculated from 1000 to 5000 micro strains.

The strength is calculated by *Equation 11* using the maximum load at failure. Then, that value is used in *Equation 9* to get τ_{12}. It may happen that because of the large axial deformation, strain gages do not survive the experiment, and the woes before failure of the specimens. However, the tensile testing machines are load and displacement control, so an approximation can be done using the machine data if there is a linear relation between the cross-head displacement of the machine, and the axial strain collected from the axial strain gage before it broke. So, the cross-head displacement (u) can be taken as an approximation of the specimen's elongation, and then divided by the specimen original length L. It should be noticed, as shown in *Equation 13*, that the cross-head displacement should be calculated as the difference between the final and initial cross-head displacement, because the starting point is different for all the specimens.

Equation 13

$$\varepsilon_u = \frac{u_f - u_i}{L}$$

The results from the In Plane shear tensile test used as an example during the chapter are shown in *Table 4*.

Table 4.

The results from the In Plane shear tensile test

Property	Value
E_x	14.02 *MPa*
ν_{xy}	0.00
$\mathbf{G_{12}I}$	3.90 *GPa*
$\mathbf{G_{12}II}$	3.92 *GPa*
$\sigma_{\mathbf{ult}}$	8.00
$\tau_{\mathbf{ult}}$	114.00
$\varepsilon_{\mathbf{ult}}$	0.11

Source: Author.

Failed specimen

Figure 26 shows a typical failed specimen from a ±45 tension test. In this case the specimen shown is from carbon fiber unidirectional *prepreg*, specifically IM7-8558. It can be seen that the specimen failed at ±45 which indicates that failure occurred mostly in the matrix. Even though it is known that during this test there is a state of biaxial tension added to the shear stress, the shear stress dominates the failure process. It can be seen by the way in which the specimen fails divided in a 45° angle each ply. Fibers oriented in the +45° and -45° are clearly visible. So, failure for the 45° specimens is shear dominated.

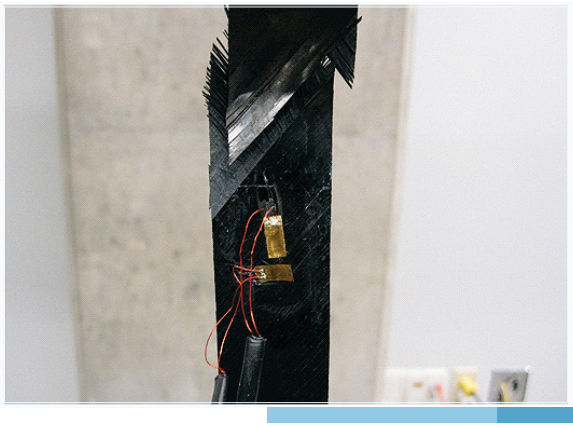

Figure 26. Failed specimen. *Source: Author.*

Figure 27. Failed specimen. *Source: Author.*

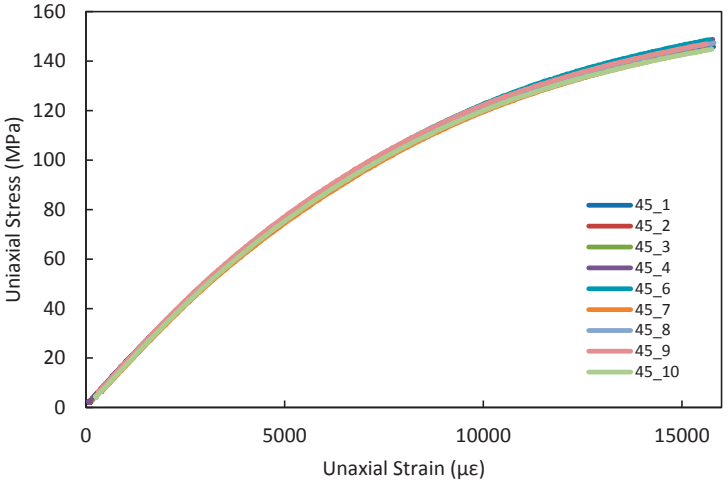

Figure 28. Typical [±45] stress vs strain plot. *Source: Author.*

A typical stress versus deformation plot is shown in *Figure 28*. The stress strain relation for $45°$ is nonlinear. For this example in particular data from the strain gages was collected up to approximately 15000 micro strains since the strain gages woes. That is why the maximum stress seems to be around $150\,MPa$ but actually specimens failed at an average stress of $228MPa$.

Conclusion

The failure in the $\pm 45°$ laminates is shear dominated. However, there is presence of a biaxial tension state of stress. For testing of composite materials a pure shear state of stress is hard to achieve, so some methods as the one explained in this chapter provide a good approximation of the shear properties of the material. The specimen deformation during this test is very high. Because of that usually, strain gauges woes and data from them can be collected up to 15000 micro strains approximately. As a result, an approximation of the ultimate strain should be taken by using the information of the crosshead displacement and the specimen original length. From the stress strain plot it could be there is no linear relation.

References

Adams, D. F., & Walrath, D. E. (1987). Current status of the Iosipescu shear test method. *Journal of Composite Materials, 21(6), 494-507.*

Adams, D. O., Moriarty, J. M., Gallegos, A. M., & Adams, D. F. (2007). The V-notched rail shear test. *Journal of composite materials, 41(3), 281-297.*

ASTM D3518M - 13. (2013). *Standard Test Method for In Plane Shear Response of Polymer Matrix Composite Materials*

by Tensile Test of a 45 Laminate. West Conshohocken, PA: American Society for Testing and Materials.

Barnes, J. A., Kumosa, M., & Hull, D. (1987). Theoretical and experimental evaluation of the Iosipescu shear test. ***Composites science and technology,*** 28(4), 251-268.

R Wisnom, M. (1995). The effect of fibre rotation in±45 tension tests on measured shear properties. ***Composites,*** 26(1), 25-32.

Sims, D. F. (1973). In-plane shear stress-strain response of unidirectional composite materials. ***Journal of Composite Materials,*** 7(1), 124-128.

Whitney, J. M. (1973). Free-edge effects in the characterization of composite materials. ***Analysis of the Test Methods for High Modulus Fibers and Composites, ASTM STP,*** 521, 167-180.

Chapter 4

Off Axis Tensile Test

Chapter 4

Off Axis Tensile Test

The off axis term refers to the fibers coordinate system being rotated at an angle θ from the specimen coordinate system. This chapter explains the procedure to perform this test and provides an example for test conducted on off axis specimens of $10°, 20°, 30°, 45°, 60°$ and $75°$. At this point, if the reader has already digested the previous chapters, it may seem boring at a glance. In fact, the testing procedure is very similar to the ones used in the previous chapters. However, this chapter brings and describes a very interesting exercise of failure prediction in composite materials, for which the information presented in Chapter 3 and Chapter 4 is necessary.

Specimen preparation

Specimens for this test should be about $230mm$ long, between 12.5 and $25mm$ wide, and the thickness should be about 6 to 8 plies of unidirectional *prepreg* (Carlsson, Adams, & Pipes, Experimental Characterization of Advanced Composite Materials, 2002) . For this kind of specimens, usually a 3 gage rectangular rosette is used as shown in *Figure 30*. It allows to completely determine the state of strain when the directions of the principal axis are unknown (TN-509, 2010).

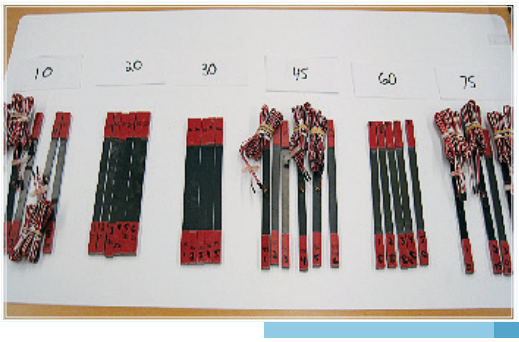

Figure 29.
Specimens. *Source: Author.*

Transverse sensitivity using a 3 gage rectangular rosette

There is an error presented on the strain gage measurements when the stress field is not uniaxial, or the gage is not parallel to the principal strain in a uniaxial stress field, or when the gage is mounted on material different from calibration material (TN-509, 2010), as is the case for this kind of tests. To account for that error, a correction should be applied to the collected data from the strain gages by the following equations:

Equation 14

$$\varepsilon_x = \frac{(1-\nu_0 K_t)(\hat{\varepsilon}_x - K_t \hat{\varepsilon}_y)}{1-K_t^2}$$

Equation 15

$$\varepsilon_y = \frac{(1-\nu_o K_t)(\hat{\varepsilon}_y - K_t \hat{\varepsilon}_x)}{1-K_t^{\,2}}$$

Equation 16

$$\varepsilon_{45} = \frac{(1-\nu_o K_t)(\hat{\varepsilon}_{45} - K_t(\hat{\varepsilon}_x + \hat{\varepsilon}_y - \hat{\varepsilon}_{45}))}{1-K_t^{\,2}}$$

Where ε_x is the corrected strain in the x direction, ε_y is the corrected strain in the y direction, ε_{45} the corrected strain in the 45 direction, K_t is the transverse sensitivity coefficient, $\hat{\varepsilon}_x$ is the indicated strain in the x direction, $\hat{\varepsilon}_y$ is the indicated strain in the y direction, $\hat{\varepsilon}_{45}$ is the indicated strain in the 45 direction, and ν_o is the Poisson's ratio for the calibration material, typically 0.285 because they are calibrated on steel.

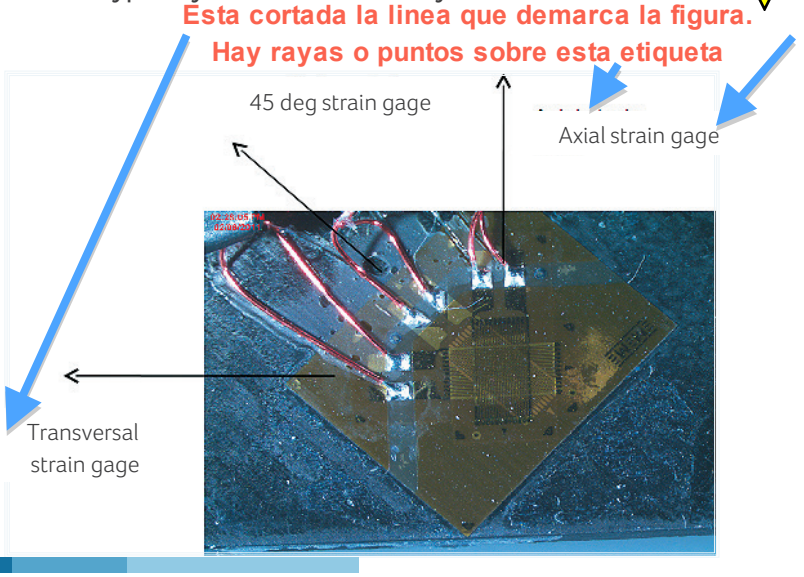

Figure 30. Strain Gage Rossete. *Source: MSE 597 report*

Materials, tools and equipment

The following materials, tools and equipment are required to obtain the properties of off axis polymer matrix composite material specimens in a tensile test:

- ***Materials***
  - » Specimens
  - » End Tabs
  - » Hysol EA 9394 or other structural adhesive

- ***Tools***

  - » Strain gages (3 x specimen)
  - » Personal protection items
  - » Caliper

- ***Equipment***

  - » Computer
  - » Data acquisition system
  - » Tensile testing machine
  - » Diamond saw or water jet

Procedure

The procedure for the off axis tensile test is as follows:

1. Design specimens as explained above
2. Manufacture panels according to Chapter 1.
3. Add the End Tabs
4. Cut panels using a diamond saw or water jet
5. Mark each specimen
6. Add transverse and longitudinal strain gages to all the coupons.
7. Measure and register each specimen thickness and width (3 measurements x specimen)
8. Calculate cross sectional area
9. Connect a strain gage (already mounted to the sample) to the data acquisition system
10. Prepare a tensile testing machine displacement controlled and the data acquisition system.
11. Clamp specimen in the tensile tester using the grips, *(see Figure 17)*. **verificar por favor si en verdad es Figura 17**
12. Test specimens at a rate of 2mm/min recording loads and displacements until failure.

Fiber orientation verification

It is recommended to do a verification of the fiber orientation using a microscope. It can be done by measuring the angle between a line parallel to the fibers and a line in the axial direction of the specimen as shown in *Figure 31.*

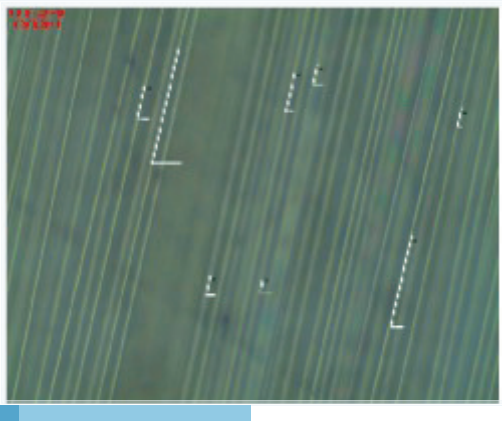

Figure 31. Angle verification. *Source: MSE 597 report.*

Failed specimens

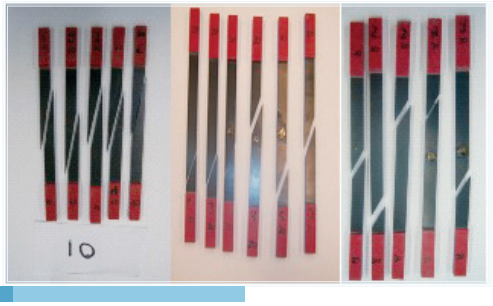

Figure 32. Typical failed specimens. *Source: Author.*

Figure 33. Typical failed specimens.
Source: Author.

Failure in the off axis unidirectional *prepreg* specimens is mostly shear dominated, especially truth for specimens with angles lower than 60 °. As shown in *Figure 32* specimens failed at the corresponding fiber orientation angle.

Failure Prediction

Maximum stress criterion

When the strength of the lamina in its principal directions 1 and 2 is known, as it was explained in Chapter 3, as well as the shear strength, as explained in Chapter 4, an interesting exercise of failure prediction can be practiced with the off axis test specimens. The state of stress in the fibers can be calculated by the use of the transformation matrix. When testing a specimen in tension, both σ_y and τ_{xy} are equal to zero because the load is applied in the specimen axial direction x. Then, by simple matrix multiplication the state of stress in the fibers coordinate system is in terms of σ_x as shown in *Equation 17*, *Equation 18* and *Equation 19*.

$$\begin{pmatrix} \sigma_1 \\ \sigma_2 \\ \tau_{12} \end{pmatrix} = \begin{pmatrix} m^2 & n^2 & 2mn \\ n^2 & m^2 & -2mn \\ -mn & mn & m^2 - n^2 \end{pmatrix} \begin{pmatrix} \sigma_x \\ \sigma_y \\ \tau_{xy} \end{pmatrix}$$

Equation 17

$$\sigma_1 = m^2\sigma_x$$

Equation 18

$$\sigma_2 = n^2\sigma_x$$

Equation 19

$$\tau_{12} = -mn\sigma_x$$

Where , $m = \cos\theta$ and $n = \sin\theta$.

From Chapter 3 and Chapter 4, the strength in the 1 and 2 direction as well as the shear strength were obtained, so σ_1, σ_2 and τ_{12} are known and solving for σ_x:

Equation 20

$$\sigma_x = \frac{\sigma_1}{m^2}$$

Equation 21

$$\sigma_x = \frac{\sigma_2}{n^2}$$

Equation 22

$$\sigma_x = -\frac{\tau_{12}}{mn}$$

Considering θ equal to zero in *Equation 20*, σ_x is equal to σ_1, which corresponds to the 0° specimen test. Similarly, θ equal to ninety in *Equation 21* corresponds to the 90° specimen test, and θ equal to forty five in *Equation 22* corresponds to the $\pm 45°$ specimen test. However, going further, plots can

made with *Equation 20*, *Equation 21* and *Equation 22* with θ values from 0 to 90, and this information can be compared with the experimental results to understand which failure mode dominates in the off axis specimen and to see if it is actually a good approximation, which is what is shown in *Figure 34*.

Tsai Wu failure criterion.

(Tsai & Wu, 1971) Published an article in 1971 where they wanted to show an operationally simple strength criterion for filamentary composites and ended up with a scalar function of two stress tensors which is still applicable. In the paper they say that they wanted to come up with something simple because what Russians workers were doing was too complicated. However, their work with not be explained in detail in this book. The criterion says that failure occurs when the left side of the equation is equal or bigger than 1.

Equation 23

$$F_{11}\sigma_{11} + F_2\sigma_{22} + F_{11}\sigma_{11}^2 + F_{22}\sigma_{22}^2 + 2F_{12}\sigma_{11}\sigma_{22} + F_{66}\tau_{12}^2 = 1$$

Where $F_1 = \frac{1}{X} + \frac{1}{X'}, F_2 = \frac{1}{Y} + \frac{1}{Y'}, F_{11} = \frac{-1}{XX'}, F_{22} = \frac{-1}{YY'}$,

$$F_{66} = \frac{1}{S^2}, \; F_{12} = -\frac{1}{2}\sqrt{F_{11}F_{22}} \text{ and.}$$

With the use of the transformation matrix to express the stresses in the fibers principal direction as a function of the stress applied to the specimen, it reduces to:

Equation 24

$$\sigma_x = \frac{1}{\sqrt{F_{11}m^4 + F_{22}n^4 + F_{66}m^2m^2 + 2F_{12}m^2m^2}}$$

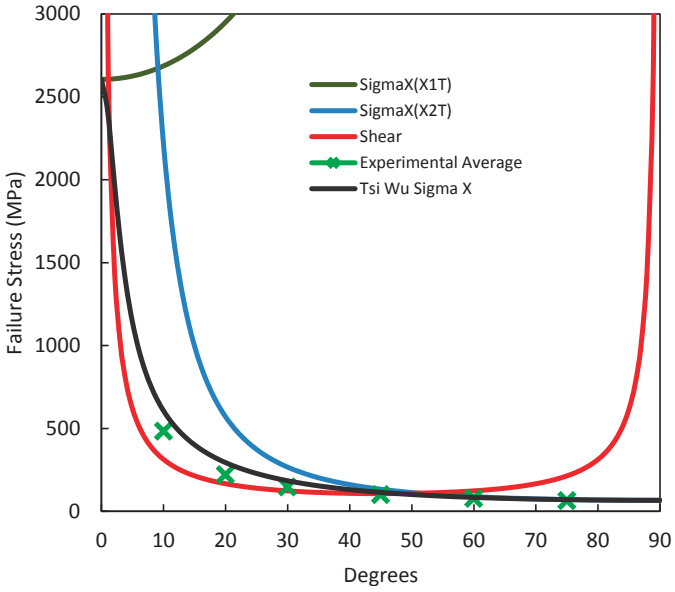

Figure 34. Failure prediction plot.
Source: Author.

It can be seen that the Tsai Wu failure criterion is a good approximation of the failure behavior of the samples. Also, for angles greater than $60°$ the tensile failure in $90°$ approximates to the experimental behavior, which means a matrix failure. For angles less than $60°$ shear failure approximates to the experimental results, which means that failure is shear dominated. The maximum stress in the 1 direction criterion is not a good approximation for failure of off axis specimens, it only applies for $0°$ specimens caused as seen in the plot, and it would indicate that off axis specimens fail at higher stresses

which is not truth. As expected, the strength decreases when the angle increases.

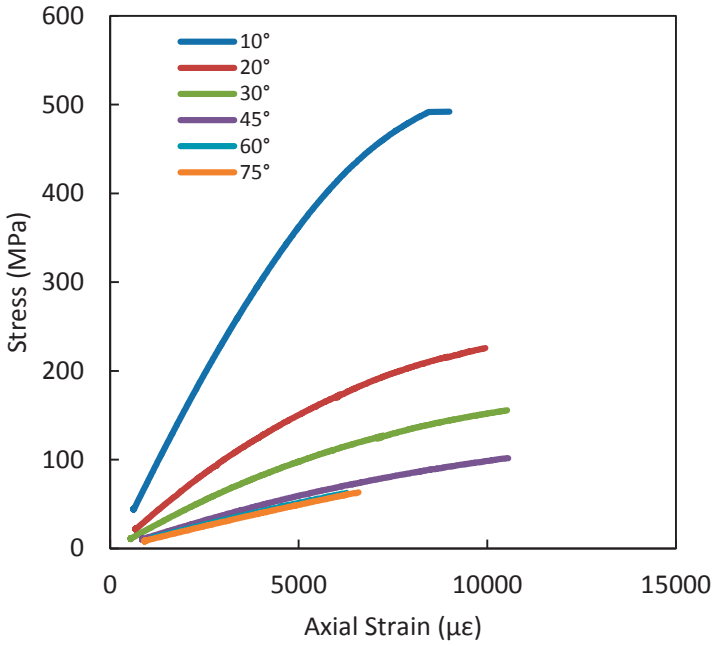

Figure 35. Stress vs strain plot. *Source: Author.*

Typical load vs deformation curves

A nonlinear stress-strain relationship can be observed in *Figure 35*. It shows that the deformation is not linear, and it is due to because during the test, the shear deformation is limited by the grips of the testing machine. As a result specimens deform in a S shape. It is important to mention that the strain gage sensitiveness correction is applied in this case.

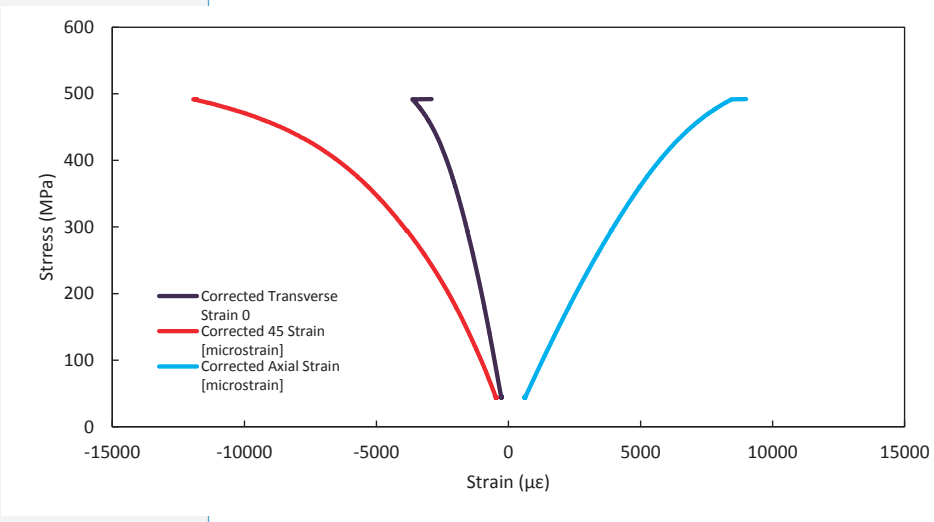

Figure 36. Stress vs strain plot with corrected strains. *Source: Author.*

Data reduction

For each specimen the following material properties can be obtained from this experiment. The Young´s modulus is obtained by:

Equation 25

$$E_x = \frac{\sigma_x}{\varepsilon_x}$$

The Poisson´s ratio by:

Equation 26

$$\nu_{xy} = \frac{-\varepsilon_y}{\varepsilon_x}$$

The coupling between shear and axial strain ratio by:

Equation 27

$$n_{xy} = \frac{\gamma_{xy}}{\varepsilon_x} = \frac{(2\varepsilon_{45} - \varepsilon_0 + \varepsilon_{90})}{\varepsilon_x}$$

And the in plane shear modulus by:

Equation 28

$$G_{12} = \frac{\tau_{12}}{\gamma_{12}} = \frac{-mn\sigma_x}{2mn(\varepsilon_y - \varepsilon_x) + (m^2 - n^2)\gamma_{xy}}$$

A summary of the results obtained during the experiments used as an example for this chapter are shown in *Table 5*.

Table 5.

Summary of experiment results

Ply Dir.	$_X$ $[GPa]$	ν_{xy}	η_{xy}	G_{12} $[GPa]$
0	156	0.339	-	-
10	81.70	0.367	-3.34	2.66
20	32.79	0.451	-3.60	1.91
30	21.00	0.423	-2.17	2.42
45	13.39	0.334	-1.39	3.76
60	10.64	0.184	-0.06	4.45
75	10.17	0.082	-0.27	7.82
90	8.46	0.018	-	-
			G12	4.31

Source: Author.

La tabla se visualiza como cortada

Conclusion

Failure in the off axis tensile test approximate to the biaxial solution done by Tsai Wu. However for small angles, generally

less than 60°, the failure is due to the shear, and for angles greater than 75°, the tensile failure of 90° approximates to the experimental results. Also, it could be seen that the coupons failed in the fiber direction.

In the off axis tensile test, coupons present a nonlinear stress strain relationship due to the grips. The shear deformation is limited because of those end constrains. As a result, the deformation of the coupons presented a *S* shape.

References

Carlsson, L. A., Adams, D. F., & Pipes, R. B. (2002). ***Experimental Characterization of Advanced Composite Materials.*** CRC Press.

TN-509. (2010). ***Errors Due to Transverse Sensitivity in Strain Gages.*** Vishay Precision Group.

Tsai, S. W., & Wu, E. M. (1971). A general theory of strength for anisotropic materials. ***Journal of composite materials,*** 5(1), 58-80.

Chapter 5

Flexural Testing in 3 Point Bending

Flexural Testing in 3 Point Bending

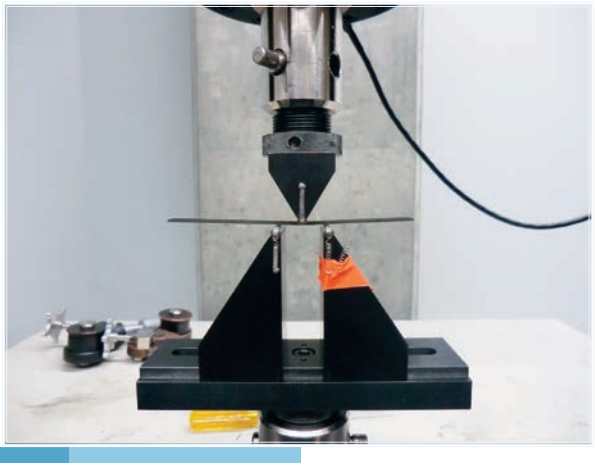

Figure 37. Flexural testing. *Source: MSE 597 report.*

Chapter 5

This chapter introduces a new kind of test: Flexural testing in 3 point bending. If a composite is designed for bending, it is appropriate to know the bending strength. Flexural bending strength and stiffness are not basic material properties; they are the result of a complex state of stress where shear, compression and bending are presented (Reis, Ferreira, Antunes, & Costa, 2007). As explained in the previous Chapters, in order to find material properties, it is necessary to expose the material to individual stress of stress, such as tension or shear. Because of this reasons, this test is not appropriate neither used to obtained basic material properties. However, it may provide an approximation of material properties as will be explained in this Chapter (Whitney & Knight, The relationship between tensile strength and flexure strength in fiber-reinforced composites, 1980). It has as an advantage, comparing to other test, that it is simple to perform, the specimen preparation is less complicated, and there is no need to clamp the specimens to the grips of a tensile testing machine.

Specimen preparation

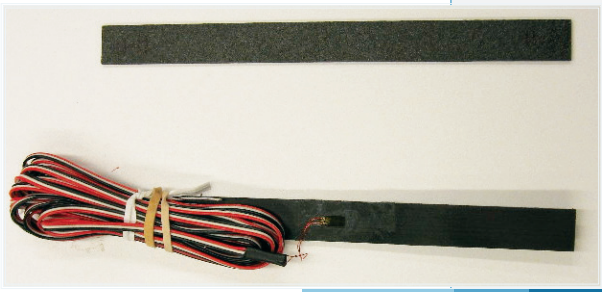

Figure 38. Typical specimen. *Source: Author.*

In order to simplify the complex state of stress, the shear is minimized by making the support span much bigger than the specimen thickness. (ASTM D6272, 2010), recommends span to thickness rations of 16, 32, and 40, to 1. (ASTM D790, 2010), recommends 32:1 or 40:1. (ASTM D7264, 2007), specifies that it should be 32:1. The latest standard also recommends the following dimensions: length 100mm, thickness 2.4mm, and width 13, for a 76.8mm span. Strain gages may replace the deflection sensing device specified on the standards. A strain gage may be installed in the bottom face of the specimen that is going to be exposed to tension, in the axial direction as shown in *Figure 38.*

Materials, tools and equipment

The following materials, tools and equipment are required for a 3 point bending flexural test of composite lamina:

- ***Materials***
  - » Specimens

- ***Tools***

  - » Strain gages (1 x specimen)
  - » Personal protection items
  - » Caliper

- ***Equipment***

  - » Computer
  - » Data acquisition system
  - » Tensile testing machine with fixture with 2 point supports as shown in *Figure 39*.
  - » Diamond saw or water jet

Procedure

The procedure to perform a flexural test by 3 point on polymer matrix reinforced composite lamina is the following:

1. Design specimens as recommended above.
2. Manufacture panels according to Chapter 1.
3. Cut panels using a diamond saw or water jet
4. Mark each specimen
5. Add a longitudinal strain gage in the specimen bottom face, or a deflection sensing device.
6. Measure and register each specimen thickness and width (3 measurements x specimen).
7. Calculate cross sectional area
8. Connect a strain gage (already mounted to the sample) to the data acquisition system
9. Prepare a testing machine displacement controlled, the support fixture, and the data acquisition system.
10. Adjust and verify the support span in the fixture.

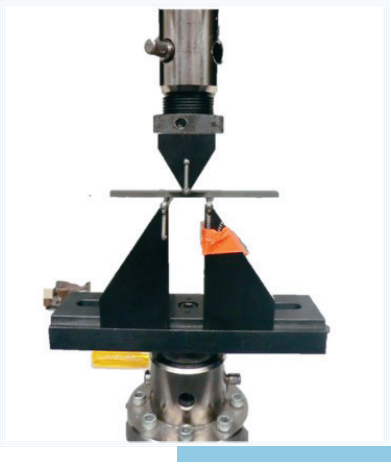

Figure 39. Testing machine with fixture. *Source: Author. Adjust and verify the support span in the fixture.*

11. Lay the specimen in the 2 supports, leaving the same length in both sides outside the supports.
12. Put the load cell in contact with the specimen until it reaches a load of approximately 10N and set it as the initial point.
13. Test specimens at a rate of 1mm/min recording loads and displacements until failure.

Data Reduction

The results were analyzed using Bernoulli beam theory (Sun C. T., 1998). This assumes that the beam is slender and long, that the deformation is low, and that there is a uniform cross sectional area. So, the stress state is dependent on the span length to specimen thickness ratio. Beams with small ratios are expected to fail due to shear and beams with big ratios are expected to fail due to tension or compression. The loading, shear, and moment diagrams for a three point flexural bending are shown in *Figure 40*.

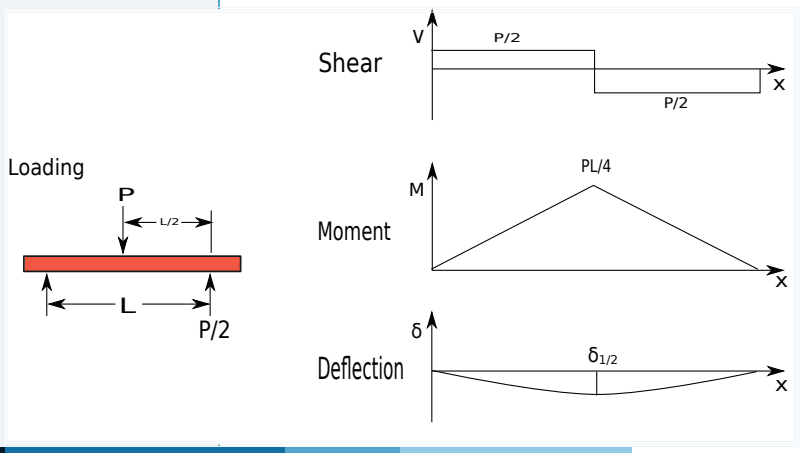

Figure 40. Shear, moment and deflection diagrams. Author.

The stress distribution on the beam is such that, the bottom surface is in tension, while the top surface is in compression. The maximum shear occurs in the middle plane and it varies parabolically being zero on the free surfaces as shown in *Figure 41*. It is express by *Equation 29* where *P* is the applied load at failure, b is the width, *h* is the thickness.

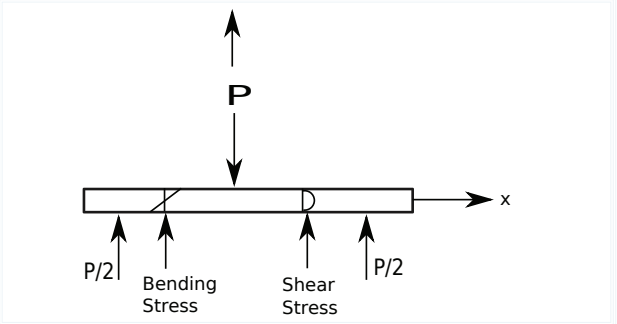

Figure 41. Stress distribution. Author.

Equation 29

$$\tau_{max} = \frac{VQ}{Ib} = \frac{3P}{2bh}$$

Maximum stress

The maximum stress occurs in the center of the beam where the moment is higher, and zero at each end support. It is expressed by *Equation 30*, where *L* is the span length, and *P* is the applied load at failure.

Equation 30

$$\sigma_{max} = \frac{Mc}{I} = \frac{3PL}{2bh^2}$$

Flexural modulus

The flexural modulus is calculated from *Equation 31*, where *P/* is the slope of the load vs deflection plot. However, it assumes that shear deformation is negligible, so in cases where shear has to be taken into account, such when there is a low span length to thickness ratio, *Equation 32* should be used.

Equation 31

$$E_f = \frac{L^3}{4bh^3}\frac{P}{\delta}$$

Equation 32

$$E_f = \frac{L^3}{4bh^3}\left[1 + \frac{6h^2E_f}{5L^2G_13}\right]\frac{\Delta P}{\Delta \delta}$$

Apparent modulus E_1 by strain gage measurements

The apparent modulus E_1 can be calculated in the specimens with strain gages, finding the slope of the stress strain plot, between 1000 - $3000\mu\varepsilon$.

Apparent modulus E_1 and shear modulus G_{13} by deflection measurements

The apparent modulus E_1 and the shear modulus G_{13} can be calculated by deflections measurements using *Equation 33*, when there are two set of data, such as tests of the same material with two different span lengths, because in that way *Equation 33* can be expressed in a matrix form shown in *Equation 34*, and it would be 2 equations and 2 unknowns. Therefore, it can be solved for the elastic constants which can be calculated since all the information needed is provided by the test.

Equation 33

$$\delta = \frac{FL^3}{48E_1I} + \frac{5FL}{6G_{12}A}$$

Equation 34

$$\begin{pmatrix} \left(\frac{\delta}{F}\right)_1 \\ \left(\frac{\delta}{F}\right)_2 \end{pmatrix} = \begin{pmatrix} \frac{L_1^3}{48I_1} & \frac{5L_1}{6A_1} \\ \frac{L_2^3}{48I_2} & \frac{5L_2}{6A_2} \end{pmatrix} \begin{pmatrix} \frac{1}{G_1} \\ \frac{1}{G_{13}} \end{pmatrix}$$

Failed specimens

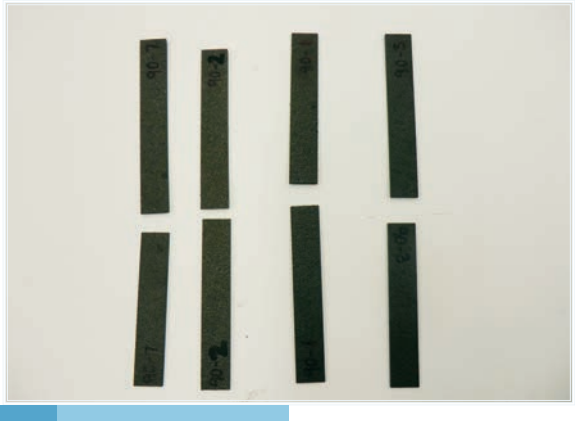

Figure 42. Typical failed specimen.
Source: Author.

Typical failed unidirectional lamina failed specimen for a 3 point bending flexural test are shown in *Figure 42*. It can be noticed that the failure occurs in the point where the load is applied.

Typical load vs deflection curves

For the purpose of explanation about the flexural behavior of unidirectional *prepreg* when loaded in a 3 point bending test, results from testing $[0]$ and $[90]$ specimens will be discussed. Test was conducted to 18 $[0]$ specimens, and 6 $[90]$ specimens. 6 $[0]$ specimens were thicker than the rest. Strain gages were installed only in 5 of $[0]$ specimens, 2 of them being the thick ones. Specimens average dimensions are shown in *Table 6*.

Table 6.

Specimen average dimensions

	0's	90's	T's
Avg. Thickness, ***mm***	1.37 ± 0.027	1.38 ± 0.0046	3.94 ± 0.047
Avg. Width, ***mm***	12.90 ± 0.05	12.85 ± 0.068	12.87 ± 0.095
Avg. Cross Section, mm^2	17.73 ± 0.39	17.76 ± 0.093	50.66 ± 0.38

Source: Author.

The $[0]$ thin specimens were tested at 3 different spans, $39.35mm$ and $50.17mm$, with $22.5:1$, $28.7:1$ and $36.6:1$, span to depth ratios respectively. The $[0]$ tick specimens and the $[90]$ specimens were tested with a span of $29.76mm$, with a span to depth ratio of $7.55:1$.

All of the [90] specimens were loaded until failure, and from the side of [0], just two of the thick ones and two of the thin ones were loaded until failure; the others were loaded until 50% of the failure load of the previous ones.

Table 7.

Testing criteria

Sample	Criteria	Span [mm]
0-4 (P=920)	failure	30,08
0-12 (P=976)	failure	30,08
0-1 (w/SG)	50%	30,08
0-2 (w/SG)	50%	30,08
0-6 (w/SG)	50%	30,08
0-7	50%	30,08
0-8	50%	39,35
0-9	50%	39,35
0-10	50%	50,17
0-11	50%	50,17
T-3	failure	29,76
T-4 (P=5730)	failure	29,76
T-2	50%	29,76
T-5	50%	29,76
T-1 (w/SG)	50%	29,76
T-7 (w/SG)	50%	29,76
90-1	failure	29,76
90-2	failure	29,76
90-4	failure	29,76
90-5	failure	29,76
90-6	failure	29,76

Source: Author.

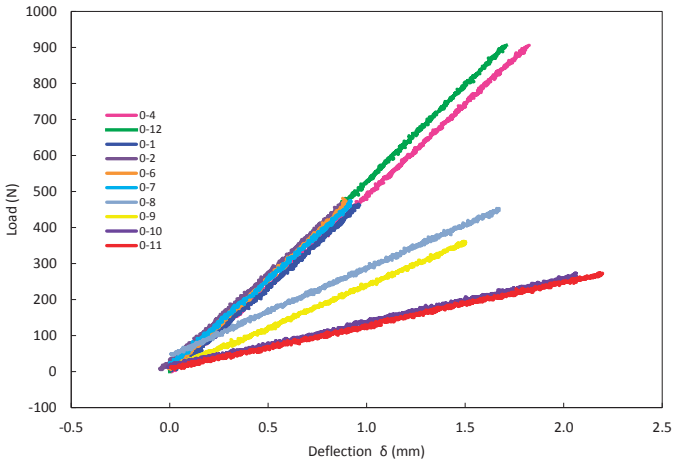

Figure 43. Load vs deflection plot for 0 thin specimens. *Source: Author.*

As shown in *Figure 43* results were as expected; the bigger the span, the higher the deflection. The red and purple lines represent the specimens with the higher span, the yellow and gray the middle span and the others the shorter span length. The green and pink lines represent the specimens that were tested until failure. The slope of the curve increases as the span length is reduced. Since the maximum flexural stress is directly proportional to the span length, it increases when the span is bigger; so, the smaller the span the stiffer the specimen.

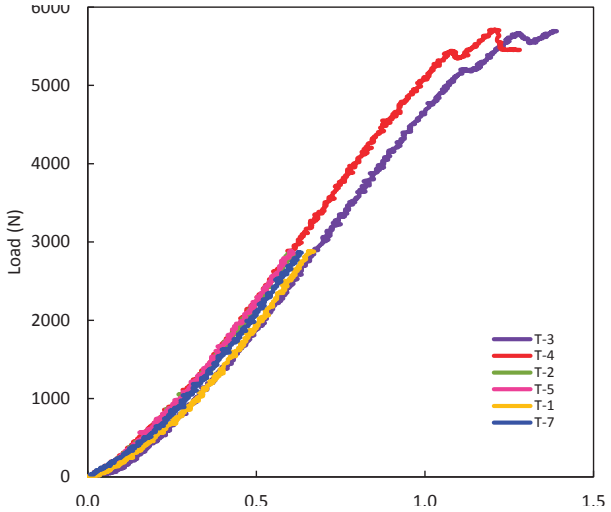

Figure 44. Load vs Deflection thick specimen. *Source: Author.*

Figure 44 shows the load deflection plot for the [0] thick specimens. The red and purple lines represent the specimens that were loaded until failure. It can be noticed that the thick [0] specimens are stiffer than the thin specimens, as it is expected. *Figure 45* and *Figure 46* show the stress vs strain plot of the specimens that had strain gages, thin and thick respectively. A slightly difference in the slopes could be observed, which means different apparent modulus.

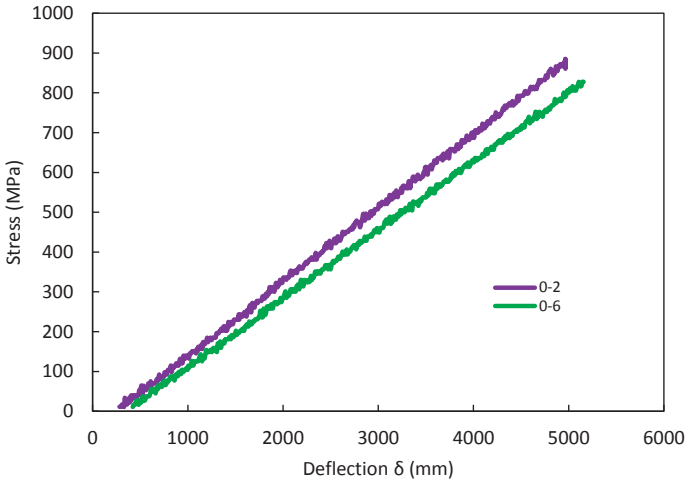

Figure 45. Stress vs strain. *Source: Author.*

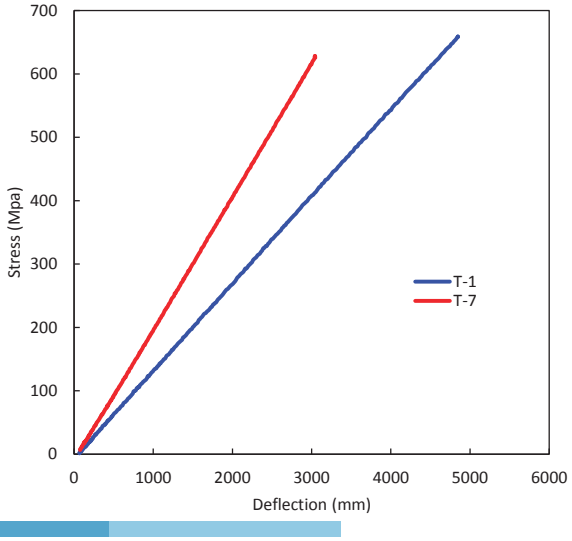

Figure 46. Stress vs strain plot for thick specimens. *Source: Author.*

Microscopy analysis

Micrographs were taken to the failure specimens. The cross sectional area of the failed specimen is shown in *Figure 47*. It can be seen that on the rough side the failure of the lamina was due to tension, while in the smooth side of the specimen the failure was due to the compression. The compression crack angles can be seen in *Figure 48* and is similar to the angle shown in *Figure 50* where a delamination due to shear can be noticed.

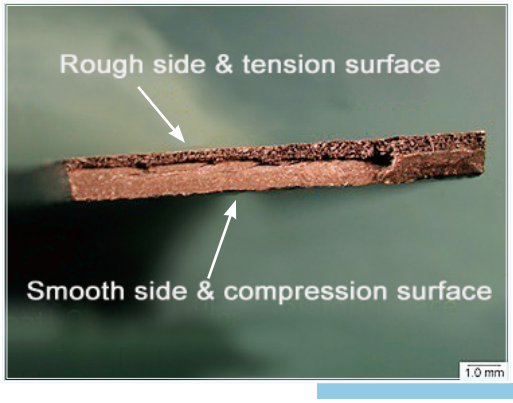

Figure 47. Micrograph showing fracture surface. *Source: MSE 597 report.*

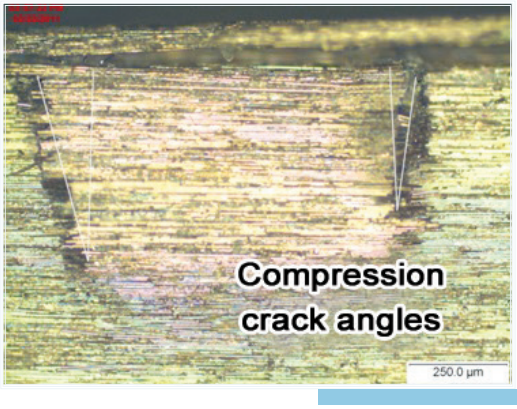

Figure 48. Compression crack angles. *Source: MSE 597 report.*

Figure 49. Compression Surface crack. *Source: MSE 597 report.*

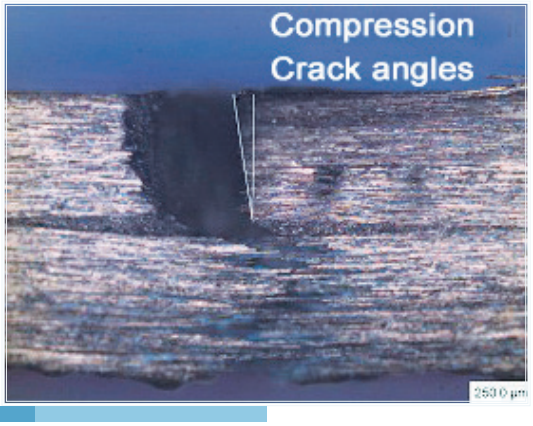

Figure 50. Failure due to compression. *Source: MSE 597 report.*

References

ASTM D6272. (2010). ***Standar Test Method for Flexural Properties of Unreinforced and Reinforced Plastics and Electrical Insulating Materials by Four-Point Bending.*** West Conshohocken, PA: American Society for Testing and Materials.

ASTM D7264. (2007). ***Standard Test Method for Flexural Properties of Polymer Matrix Composite Materials.*** American Society for Testing and Materials.

ASTM D790. (2010). ***Standard Test Methods for Flexural Properties of Unreinforced and Reinforced Plastics and Electrical Insulating Materials.*** West Conshohocken, PA: American Society for Testing and Materials.

Reis, P. N., Ferreira, J. A., Antunes, F. V., & Costa, J. D. (2007). Flexural behaviour of hybrid laminated composites. ***Composites Part A: Applied Science and Manufacturing,*** 38(6), 1612-1620.

Sun, C. T. (1998). ***Mechanics of aircraft structures.*** Wiley.

Whitney, J. M., & Knight, M. (1980). The relationship between tensile strength and flexure strength in fiber-reinforced composites. ***Experimental Mechanics,*** 20(6), 211-216.

Chapter 6

Lamina Thermoelastic Response

Lamina Thermoelastic Response

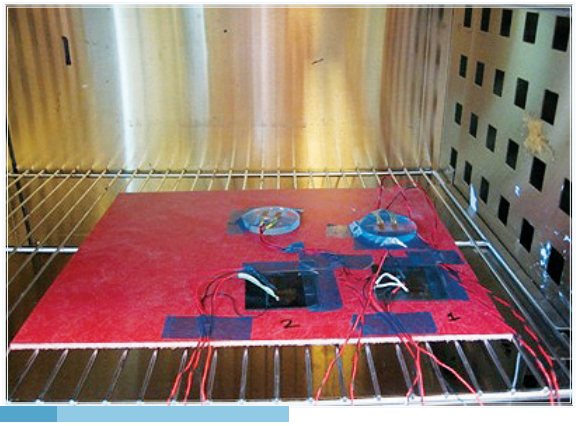

Figure 51. Lamina thermo-elastic set up. *Source:Author.*

A structure or part of a structure may be Lamina of a composites material, which during its use may be exposed to gradients of temperature. Thus, it is necessary to know its changes in dimensions with respect to the changes in temperature to confirm its applicability for specific uses. This relation is known as the coefficient of thermal expansion. This chapter explains how to obtain it for a composite lamina using the strain gage method (di Scalea, 1998).

Chapter 6

Materials, tools and equipment

The following materials, tools and equipment are required to obtain the lamina thermoelastic response by the strain gage method:

- ***Materials***
  - » Specimens
  - » Reference specimen

- ***Tools***

  - » Strain gages (2 x specimen)
  - » Temperature gauge (1 x specimen)
  - » Personal protection items
  - » Caliper

- ***Equipment***

  - » Computer
  - » Data acquisition system
  - » Temperature controlled convection oven
  - » Diamond saw or water jet

Procedure

1. Design an 8 ply unidirectional laminate
2. Fabricate laminate 2 panels as explained in Chapter 1.
3. Cut panels using a diamond saw or water jet
4. Mark each specimen
5. Add a 0-90º strain gauge rosette and a temperature gage to each specimen.
6. Prepare the reference specimen and add strain gages to it. Each laminate must have its own reference specimen, as shown in *Figure 52*.

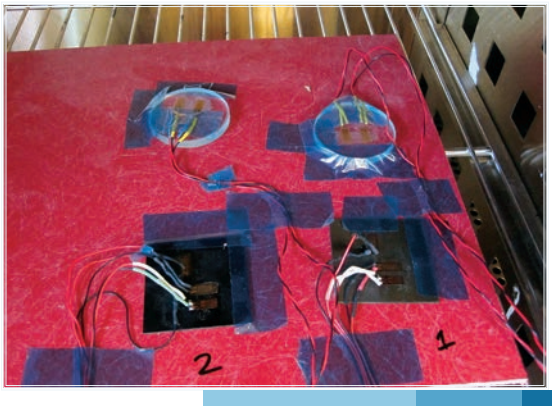

Figure 52. Set up for laminate thermoelastic response. *Source: Author.*

7. Connect a strain and temperature gages (already mounted to the sample) to the data acquisition system
8. Prepare a temperature controlled convection oven, and the data acquisition system.
9. Put the laminates and reference specimens on the oven.
10. Close and secure the oven.
11. Heat up the oven at a rate of 5°C/min starting from room temperature until 100°C, recording temperatures and strains during the whole test.
12. Allow it to cool down until room temperature is reached again.

Figure 53. Test equipment. *Source: Author.*

The reason for using a reference specimen is because the raw data collected from the strain gauges is affected by factors such as the gauge dimensions and resistance changes with temperature, gauge transverse sensitivity, and gauge factor changes with temperature (TN-513-1, 2010). A correction is applied when using the same strain gauges mounted in all specimens during the test, since the factors are expected to be consistent for the same kind of gauges.

As an example for this Chapter an experiment carried on two 8 ply, unidirectional IM7-8552 Laminate plates will be explained. As stated in the procedure, panels were fabricated according to Chapter 1, and a 0-90º strain gauge rosette and a temperature gauge were mounted on each laminate to measure the strains and temperature respectively. In addition, a reference specimen mounted with two strain gauges was used for the set up. The reference specimen was quartz whose Coefficient of Thermal Expansion CTE is 0.56 /Cº. A temperature controlled convection oven, Lindberg Blue/M was used for the test. Specimens were heated up in the oven at a rate of 5°C/min from room temperature to 100°C, and then cooled down until room temperature was reached again. Temperature and strain from all the gauges was collected throughout the entire test.

Data Reduction

The coefficients of thermal expansion in the lamina were calculated using the data from the test and compared with the results obtained by a micromechanics approach.

Test coefficient of thermal expansion calculation

The change in gauge resistance is given by *Equation 1* and *2*, where $\Delta R/R$ is the relative change in resistance, α_c and α_g are the coefficient of thermal expansion of the composite and reference material respectively, S_g is the gage factor, ΔT is the temperature change, and γ is the temperature coefficient of resistivity of the gage material.

Equation 35

$$\frac{\Delta R_1}{R} = \left(\alpha_c - \alpha_g\right) S_g \Delta T + \gamma \Delta T$$

Equation 36

$$\frac{\Delta R_2}{R} = \left(\alpha_r - \alpha_g\right) S_g \Delta T + \gamma \Delta T$$

Adding *Equation 1* and 2 we obtain *Equation 3*, where ε_c and ε_r are the strains of the composite and reference material.

Equation 37

$$\alpha_c = \alpha_r + \frac{(\varepsilon_c - \varepsilon_r)}{\Delta T} = \alpha_r + \frac{\Delta \varepsilon_A}{\Delta T}$$

Then, using the Wheatstone Half Bridge (Hoffmann, 2001) shown in *Figure 4*, the apparent difference in strains $\varepsilon_c - \varepsilon_r$, can be calculated to get the true strain in the composite ε_c by *Equation 4*, where ε_A is the apparent strain.

Equation 38

$$\varepsilon_c = \alpha_r \Delta T + \varepsilon_A$$

The true strain is represented for both the axial and transverse direction by ε_1 and ε_2 respectively. The slope of the curve ε_1 and ε_2 versus temperature T is the correspondent coefficient of thermal expansion, and can be expressed by *Equation 5* and 6.

Equation 39

$$\alpha_1 = \frac{\Delta \varepsilon_1}{\Delta T}$$

Equation 40

$$\alpha_2 = \frac{\Delta \varepsilon_2}{\Delta T}$$

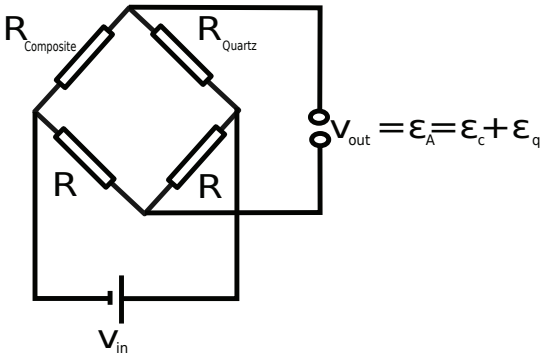

Figure 54. Wheatstone Half Bridge. *Author: MSE report.*

Micromechanics coefficient of thermal expansion calculation

The coefficient of thermal expansion can be calculated also using the micromechanics approach by the use of the self-consistent field relation in *Equation 7* and *8*.

Equation 41

$$\alpha_1 = \frac{\alpha_{1f} E_{1f} V_f + \alpha_m E_m V_m}{E_{1f} V_f + E_m V_m}$$

Equation 42

$$\alpha_2 = \alpha_3 = \left(\alpha_{2f} + \nu_{12f}\alpha_{1f}\right)V_f + \alpha_m\left(1+\nu_m\right)\left(1-V_f\right) - \left[\nu_{12f}V_f + \nu_m V_m\right]\left[\frac{\alpha_{1f}E_{1f}V_f + \alpha_m E_m V_m}{E_{1f}V_f + E_m V_m}\right]$$

α_{1f}, α_{2f} and α_m are the coefficient of thermal expansion of the fiber and matrix, E_{1f} and E_m are the Young's Modulus, ν_{12f} and ν_m are the Poisson's ratios, and V_f is the fiber volume fraction and V_m is the matrix volume fraction.

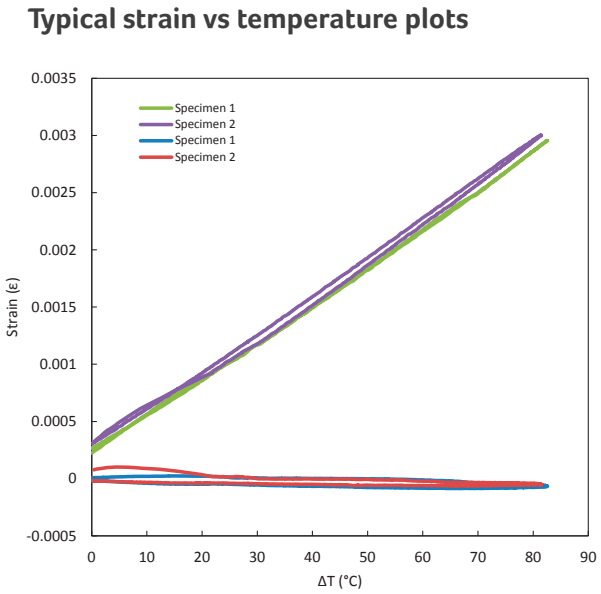

Figure 55. Strain vs. Temperature plot from run 1. *Source: Author.*

A typical strain versus temperature plot from a lamina thermoelastic test is as shown in *Figure 55*. It shows results from the test used as example. Results were as expected. Six out of seven runs done were successful. Data from one of the run was not used since it was stopped short. It can be seen that the slope is higher in the transverse direction than in the axial direction. So, the coefficient of thermal expansion in the transverse direction is higher than in the axial direction. In the axial direction the slope is almost zero.

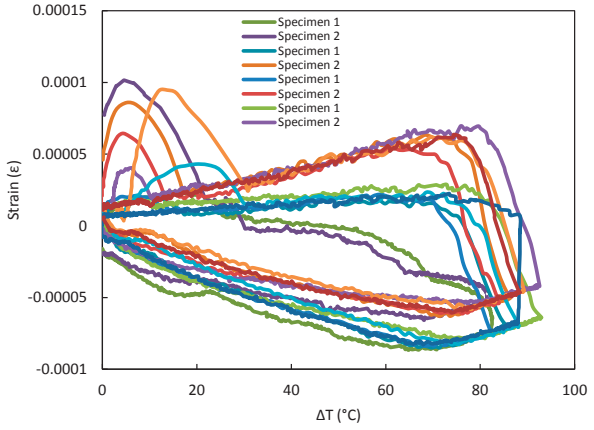

Figure 56. Strain vs delta T. *Source: Author.*

The hysteresis (di Scalea, 1998) effect is visible in both transverse and axial direction. However it is larger in the axial direction as shown in *Figure 56*. It may be due to the fact that the axial coefficient of thermal expansion is of the same order as the reference sample, and as a consequence noise is generated.

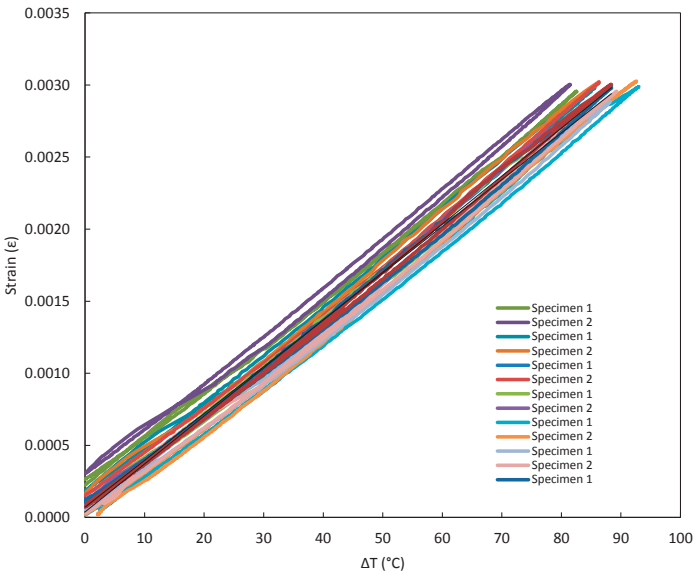

Figure 57.
Transversal Strain vs. Temperature plot.
Source: Author.

The Coefficients of thermal expansion obtained through the test are shown in *Table 8*.

Table 8.

IM7 8552 CTE

		$\alpha_1(\mu\varepsilon/°C)$	$\alpha_2\ (\mu\varepsilon/°C)$
run 4	specimen 1	-0.851	32.1
	specimen 2	-0.631	32.9
run 5	specimen 1	-0.765	32.4
	specimen 2	-0.499	33.3
run 6	specimen 1	-0.800	32
	specimen 2	-0.509	32.9
run 7	specimen 1	-0.754	33.3
	specimen 2	-0.599	32.5
average		-0.676	32.7
standard deviation		0.135	0.504

Source: Author.

Micromechanics coefficient of thermal expansion

Coefficient of thermal expansion can also be calculated by a micromechanics approach. To do so, it is necessary to know the matrix and fiber properties. The matrix and fiber properties used for the calculation of the Coefficient of Thermal Expansion with micromechanics theory are shown in *Table 9*. The coefficient of thermal expansion in the fiber direction α_1 was , $-0.394\ \mu\varepsilon/°C$ and in the transverse direction α_2 was $42.8\ \mu\varepsilon/°C$.

Table 9.

Material Properties used for Micromechanics calculations

	α_1 (strain/°C)	α_2 (strain/°C)	E_1 (GPa)	ν_{12}	Volume Fraction
Fiber	-4.00E-07	5.60E-06	276	0.28	0.5503
Matrix	6.48E-05	6.48E-05	4.76	0.37	0.4497

Source: Author.

The variation of the Coefficients of Thermal Expansion with respect to the volume fraction is shown in *Figure 58*. The x axis represents the fiber volume fraction, and the y axis the CTE. The matrix volume fraction for the calculations is taken as the difference of the fiber volume fraction with the unity. It can be seen that for approximately at a Fiber Volume Fraction of 0.65 and its corresponding matrix volume fraction of 0.35, the micromechanics results approach to the experimental results.

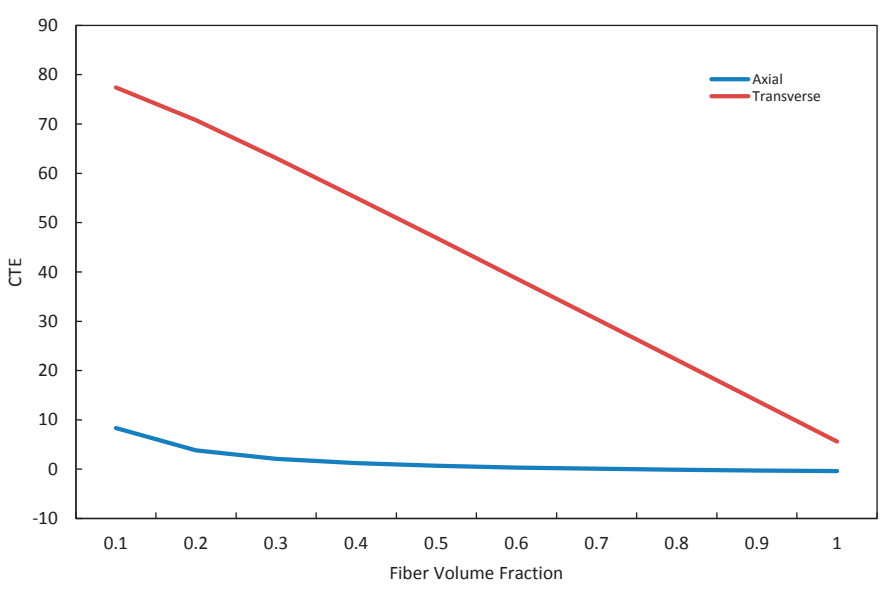

Figure 58. CTE v. Fiber Volume Fraction. *Source: Author.*

Results Comparison

A comparison of the results is shown in *Table 10*. It can be noticed that the fiber volume fraction has a large effect in the predicted values. However, the volume fractions used for the calculation were not the actual volume fraction of the specimens. The axial coefficient of thermal expansion is just a representation since its true value is within the noise of the reference specimen.

Table 10.

Results comparison

	Predicted Value	Experimental Value	Percent Difference
$\alpha_1(\mu\varepsilon / °C)$	-0.39	-0.676	126%
$\alpha_2(\mu\varepsilon / °C)$	42.78	32.7	31%

Source: Author.

Conclusions

The coefficients of thermal expansion in the axial and transverse direction of two composites lamina specimens were discussed. Results from an experiment were used as an example during the chapter. These results were compared with prediction of the properties by a micromechanics approach.

The comparison between both results showed a large percentage of difference. However, it should be noticed that the volume fraction do not correspond to the specimen's actual values, and that the values for the axial CTE are within the noise, which increases the percentage of difference.

The axial coefficient of thermal expansion α_1 is almost equal to zero, and smaller than the transverse coefficient of thermal expansion. As a result, when exposed to change of temperatures the axial dimensions in a lamina will remain almost the same, while in the transverse direction a variation in dimensions will occur.

Hysteresis effect was presented in both axial and transverse calculations. However, the effect was larger in the axial CTE. The reason is that the axial CTE of the reference material is of the same order, which produces noise. This could be

solved by using a reference material with lower coefficient of thermal expansion, or by using other method to calculate the CTE. Though, other methods used to calculate the Coefficients of Thermal Expansion are much more expensive.

References

Di Scalea, F. L. (1998). Measurement of thermal expansion coefficients of composites using strain gages. *Experimental Mechanics,* 38(4), 233-241.

Hoffmann, K. (2001). Applying the Wheatstone Bridge Circuit. *HBM S1569-1.1 .*

TN-513-1. (2010). *Measurement of Thermal Expansion Coefficient Using Strain Gages.* Vishay Precision Group.

Chapter 7

Laminate Thermoelastic Response

Laminate Thermoelastic Response

Figure 59. Laminate thermoelastic response. *Source: Author.*

Chapter 7

Some of the applications of composite materials involve high temperature changes, or the capability to stand extreme temperatures, such as in engines or turbines, and the space shuttle. Thus, the variation in dimensions with respect to the change in temperature, usually known as coefficient of thermal expansion, must be evaluated. Each laminate has its own coefficient of thermal expansion.

Unsymmetrical and not balanced composite laminates present out of plane deflection as a result of the moments generated in the laminate (Sun & Liao, 1990). This makes the coefficient of thermal expansion calculation complex. However, when dealing with symmetric and balance laminates, they can be treated as homogeneous orthotropic material. There are different methods to determine the coefficient of thermal expansion; however, this chapter focuses on the strain gage method (TN-513-1, 2010).

Materials, tools and equipment

The following materials, tools and equipment are required to obtain the laminate thermoelastic response by the strain gage method:

- ***Materials***
  - » Specimens
  - » Reference specimen
- ***Tools***
  - » Strain gages (2 x specimen)
  - » Temperature gage (1 x specimen)
  - » Personal protection items
  - » Caliper
- ***Equipment***
  - » Computer
  - » Data acquisition system
  - » Temperature controlled convection oven
  - » Diamond saw or water jet

Procedure

1. Define the laminate stacking sequence to analyze.
2. Fabricate laminate panels as explained in Chapter 1.
3. Cut panels using a diamond saw or water jet
4. Mark each specimen
5. Add a 0-90º strain gauge rosette and a temperature gage to each specimen.
6. Prepare the reference specimen and add strain gages to it. Each laminate must have its own reference specimen, as shown in *Figure 52*.

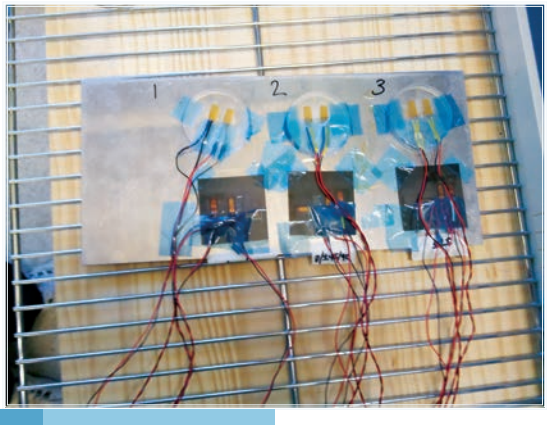

Figure 60. Set up for laminate thermoelastic response. *Source: Author.*

7. Connect a strain and temperature gages (already mounted to the sample) to the data acquisition system
8. Prepare a temperature controlled convection oven, and the data acquisition system.
9. Put the laminates and reference specimens on the oven.
10. Close and secure the oven.
11. Heat up the oven at a rate of 5°C/min starting from room temperature until 100°C, recording temperatures and strains during the whole test.
12. Allow it to cool down until room temperature is reached again.

Figure 61. Test equipment. *Source: MSE 597 report.*

As explained in the previous Chapter, the reason for using a reference specimen is because the raw data collected from the strain gauges is affected by several factors such as the gauge dimensions and resistance changes with temperature, gauge transverse sensitivity, and gauge factor changes with temperature (TN-513-1, 2010). A correction is applied when using the same strain gauges mounted in all specimens during the test, since the factors are expected to be consistent for the same kind of gauges.

Data Reduction

The coefficients of thermal expansion in the laminate are calculated using the data from the test. In addition, experimental results can be compared with laminate plate theory. The change in gage resistance is given by *Equation 43* and *Equation 44*, where $\frac{\Delta R}{R}$ is the relative change in resistance, α_c and α_g are the coefficient of thermal expansion of the composite and reference material respectively, S_g is the gage factor, ΔT is the temperature change, and γ is the temperature coefficient of resistivity of the gage material.

Equation 43

$$\frac{\Delta R_1}{R} = \left(\alpha_c - \alpha_g\right) S_g \Delta T + \gamma \Delta T$$

Equation 44

$$\frac{\Delta R_2}{R} = \left(\alpha_r - \alpha_g\right) S_g \Delta T + \gamma \Delta T$$

Adding *Equation 1* and *2* we obtain *Equation 3*, where ε_c and ε_r are the strains of the composite and reference material.

Equation 45

$$\alpha_c = \alpha_r + \frac{(\varepsilon_c - \varepsilon_r)}{\Delta T} = \alpha_r + \frac{\Delta \varepsilon_A}{\Delta T}$$

Then, using the Wheatstone Half Bridge shown in *Figure 4*, the apparent difference in strains $\varepsilon_c - \varepsilon_r$ can be calculated to get the true strain in the composite ε_c by *Equation 4*, where is the apparent strain.

Equation 46

$$\varepsilon_c = \alpha_r \Delta T + \varepsilon_A$$

The true strain is represented for both the axial and transverse direction by ε_x and ε_x respectively. The slope of the curve ε_x and ε_x versus temperature T is the correspondent coefficient of thermal expansion, and can be expressed by *Equation 5* and *6*.

Equation 47

$$\alpha_x = \frac{\Delta \varepsilon_x}{\Delta T}$$

Equation 48

$$\alpha_y = \frac{\Delta \varepsilon_y}{\Delta T}$$

Laminate Plate theory *coefficient of thermal expansion calculation*

The coefficient of thermal expansion is also calculated using laminate plate theory with the following expressions:

Equation 49

$$\begin{bmatrix} N_x + N_x^T \\ N_y + N_y^T \\ N_{xy} + N_{xy}^T \end{bmatrix} = \begin{bmatrix} A_{11} & A_{12} & A_{16} \\ A_{12} & A_{22} & A_{26} \\ A_{16} & A_{26} & A_{66} \end{bmatrix} \begin{bmatrix} \varepsilon_x^0 \\ \varepsilon_y^0 \\ \gamma_{xy}^0 \end{bmatrix} + \begin{bmatrix} B_{11} & B_{12} & B_{16} \\ B_{12} & B_{22} & B_{26} \\ B_{16} & B_{26} & B_{66} \end{bmatrix} \begin{bmatrix} N_x + N_x^T \\ N_y + N_y^T \\ N_{xy} + N_{xy}^T \end{bmatrix} = \begin{bmatrix} A_{11} & A_{12} & A_{16} \\ A_{12} & A_{22} & A_{26} \\ A_{16} & A_{26} & A_{66} \end{bmatrix} \begin{bmatrix} \varepsilon_x^0 \\ \varepsilon_y^0 \\ \gamma_{xy}^0 \end{bmatrix} + \begin{bmatrix} B_{11} & B_{12} & B_{16} \\ B_{12} & B_{22} & B_{26} \\ B_{16} & B_{26} & B_{66} \end{bmatrix} \begin{bmatrix} K_x \\ K_y \\ K_{xy} \end{bmatrix}$$

Equation 50

$$\begin{bmatrix} M_x + M_x^T \\ M_y + M_y^T \\ M_{xy} + M_{xy}^T \end{bmatrix} = \begin{bmatrix} B_{11} & B_{12} & B_{16} \\ B_{12} & B_{22} & B_{26} \\ B_{16} & B_{26} & B_{66} \end{bmatrix} \begin{bmatrix} \varepsilon_x^0 \\ \varepsilon_y^0 \\ \gamma_{xy}^0 \end{bmatrix} + \begin{bmatrix} D_{11} & D_{12} & D_{16} \\ D_{12} & D_{22} & D_{26} \\ D_{16} & D_{26} & D_{66} \end{bmatrix} \begin{bmatrix} K_x \\ K_y \\ K_{xy} \end{bmatrix}$$

Where

$$A_{ij} = \sum_{k=1}^{N} Q_{ij}^{'} \left(z_k - z_{k-1} \right)$$

$$B_{ij} = \frac{1}{2} \sum_{k=1}^{N} Q_{ij}^{'} \left(z_k^2 - z_{k-1}^2 \right)$$

N^T Thermal force resultant

M^T Thermal moment resultant

$\varepsilon_x^0, \varepsilon_y^0, \gamma_{xy}^0$ Midplane strains

K_x, K_y, K_{xy} Curvatures

Then, expressing the above equation in a short form:

Equation 51

$$\begin{bmatrix} N \\ M \end{bmatrix} = \begin{bmatrix} A & B \\ B & D \end{bmatrix} \begin{bmatrix} \varepsilon^0 \\ k \end{bmatrix}$$

And solving for the displacements:

Equation 52

$$\begin{bmatrix} \varepsilon^0 \\ k \end{bmatrix} = \begin{bmatrix} A^{'} & B^{'} \\ B^{'} & D^{'} \end{bmatrix} \begin{bmatrix} N \\ M \end{bmatrix}$$

For a symmetric and balanced laminate the B matrix, the thermal resultant moments, and A_{16} and A_{26} terms, are equal to zero. That means there is not out of plane deflexion in the laminate. So, the strains can be calculated by

Equation 53

$$\begin{bmatrix} \varepsilon_x \\ \varepsilon_y \\ \gamma_{xy} \end{bmatrix} = \begin{bmatrix} A_{11}^{'} & A_{12}^{'} & 0 \\ A_{12}^{'} & A_{22}^{'} & 0 \\ 0 & 0 & A_{11}^{'} \end{bmatrix} \begin{bmatrix} N_x^T \\ N_y^T \\ 0 \end{bmatrix}$$

It should be noticed that the in plane shear resultant force N_{xy}^T is equal to zero. As a result, the in-plane shear deformation is also equal to zero. CTE is expressed by *Equation 54*, substituting the strain expressions from *Equation 11*:

Equation 54

$$\alpha_x = \frac{A_{11}^{'} N_x^T + A_{12}^{'} N_y^T}{\Delta T}$$

Equation 55

$$\alpha_y = \frac{A_{12}^{'} N_x^T + A_{22}^{'} N_y^T}{\Delta T}$$

Where $A_{11}^{'} = \frac{A_{22}}{A_{11}A_{22} - A_{12}^2}$, $A_{12}^{'} = \frac{-A_{12}}{A_{11}A_{22} - A_{12}^2}$, $A_{22}^{'} = \frac{A_{11}}{A_{11}A_{22} - A_{12}^2}$

Typical strain vs temperature curves

Test coefficient of thermal expansion

$[0/\pm 45/0]_s$, $[0/\pm 45/90]_s$ and $[\pm 25]_{2s}$ IM7-8552 Laminate plates are used as an example for this Chapter. A $0-90^{\circ}$ strain gauge rosette and a temperature gauge were mounted on each laminate to measure the strains and temperature respectively. In addition, a reference specimen mounted with two strain gau-

ges was used for the set up. The reference specimen was quartz whose Coefficient of Thermal Expansion CTE is $0.56\frac{\mu\varepsilon}{C^0}$. The results from the test were as expected. A sample of the plots is shown in *Figure 62*. A linear fit was done using all the data. The sample correspond to the $[0/\pm45/0]_s$ laminate. It can be seen that the slope is higher in the transverse direction than in the axial direction. So, the coefficient of thermal expansion in the transverse direction is higher than in the axial direction. In the axial direction the slope is almost zero. It also means that the $0°$ plies are dominant in the axial deformation of the laminate.

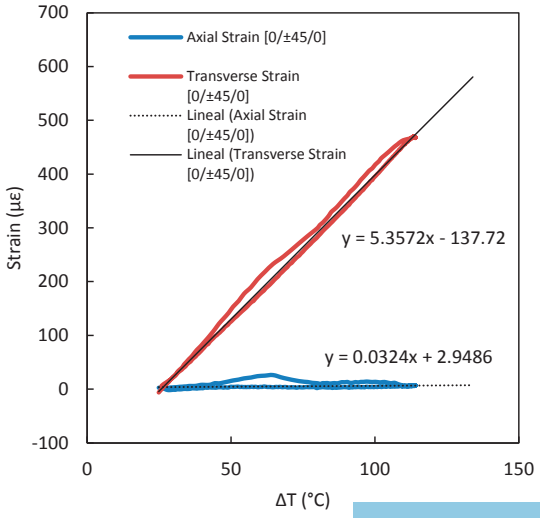

The hysteresis effect is visible in both transverse and axial direction. However it is larger in the axial direction. It may be due to the fact that the axial coefficient of thermal expansion is of the same order as the reference sample, and as a consequence noise is generated. The hysteresis effect can also be represented in the percentage of difference between the CTE calculated with the linear fit of all the data, versus the CTE calculated just with the linear fit from the heating or cooling data respectively, as shown in *Table 11*. It shows that there is a large difference on the results depending on which data is used for the analysis, and also that the hysteresis is higher in the axial CTE than in the transverse.

Figure 62. Strain vs. Temperature sample plot. *Source: MSE 597 report.*

Table 11.
***CTE* Comparison**

	Specimen	Entire Cycle	Heating	Cooling	%Difference	
					Heating	Cooling
$\alpha_1(\mu\varepsilon/°C)$	$[0/\pm45/0]_s$	0.0498	0.0307	0.0718	38.4	-44.2
	$[0/\pm45/90]_s$	1.5768	1.3934	1.6943	11.6	-7.5
	$[\pm25]_{2s}$	3.0445	3.0196	3.1036	0.8	-1.9
$\alpha_2(\mu\varepsilon/°C)$	$[0/\pm45/0]_s$	5.2452	5.5046	4.82	-4.9	8.1
	$[0/\pm45/90]_s$	1.5796	1.4267	1.6812	9.7	-6.4
	$[\pm25]_{2s}$	18.758	18.765	18.711	-0.04	0.3

Source: MSE 597 report.

From the experimental results, it can be seen that: For the case of the $[0/\pm45/0]_s$ laminate, the *CTE* is higher in the transverse direction than in the axial direction; For the $[0/\pm45/90]_s$ the *CTE* are almost the same in both direction, presenting a kind of isotropic property for this particular laminate; For the $[\pm25]_s$ the *CTE* is higher in the transverse direction than in the axial direction, and besides, they are much more higher compering with the *CTE* of the other laminates. This again shows the dominance of the $0°$ plies on each laminate.

Laminate Plate Theory coefficient of thermal expansion

The Laminate Plate theory results were obtained using the properties shown in *Table 12*.

Table 12.

Lamina properties used for calculations

Property	Value
E_1	$156.6\,GPa$
E_2	$8.5\,GPa$
ν_{12}	0.34
G_{12}	$3.9\,GPa$
α_1	$-0.676\,\mu\varepsilon\,/\,°C$
α_2	$32.7\,\mu\varepsilon\,/\,°C$
h_0	$0.17\,mm$
T_i	$20°C$
T_f	$120°C$

Source: Author.

The results comparison is shown in *Table 13*. The difference between the experimental and predicted results may be due to the fact that the CTE for the previous year lab were used for the analysis with these year's mechanical properties. Besides, the inputs in NANOhub were the average values. Moreover, there is a thermal conductivity difference between the composite samples and the quartz samples that can interfere in the results.

Table 13.

Results comparison

	$\alpha_1(\mu\varepsilon/°C)$		$\alpha_2(\mu\varepsilon/°C)$	
	Experimental	**Predicted**	**Experimental**	**Predicted**
$[0/\pm45/0]_s$	0.064±0.038	–1.097	5.31±0.063	8.24
$[0/\pm45/90]_s$	1.631±0.038	1.549	1.664±0.087	1.549
$[\pm25]_{2s}$	3.094±0.046	–5.49	18.376±0.260	25.14

Source: Author.

The percentage of error for each specimen is shown in *Table 14*. It can be seen that the percentage of error are very high. However the $[0/\pm45/90]_s$ laminate presented the lowest percentage errors for both axial and transverse CTE .

Table 14.

Error comparison

Specimen	Error % $\acute{a}_x$	Error % $\acute{a}_y$
$[0/\pm45/0]_s$	94.2	-35.6
$[0/\pm45/90]_s$	5.3	7.4
$[\pm25]_s$	-161.3	-27.0

Source: Author.

Conclusions

The coefficients of thermal expansion in the axial and transverse direction of two composites lamina specimens were defined. An example used provided results which were compared with prediction of the properties by Laminate Plate Theory. The coefficients of thermal expansion in the laminate are influenced strongly by the presence of $0°$ plies. The more $0°$ plies a laminate contains in certain direction, the more the CTE in that direction approaches to zero. It could be seen that the $[0/\pm 45/90]_s$ laminate present an isotropy property, since the CTE in the axial and transverse direction were almost the same according with the experimental results, and exactly the same according to the predicted values.

Hysteresis effect was presented in both axial and transverse calculations. However, the effect was larger in the axial CTE. When calculating the CTE just with the heating or cooling data and compering with the results when calculating with all the data, it could be seen that the difference was higher in the axial CTE. However, it also shows that a variation in the results depending on the data taken for the analysis.

References

Sun, C. T., & Liao, W. C. (1990). Analysis of thick section composite laminates using effective moduli. *Journal of Composite Materials,* 24(9), 977-993.

TN-513-1. (2010). Measurement of Thermal Expansion Coefficient Using Strain Gages. *Vishay Precision Group.*

Chapter 8

Open Hole Tensile Test

Open Hole Tensile Test

Figure 63. Open Hole Tensile Test. Source: Author.

Chapter 8

Tensile strength of notched laminates has been studied since notched components are one of the design drivers of composites structures (Cruse, 1973). The decrease in the strength of the laminate when increasing the hole size is known as the "Size Hole Effect" (Nuismer & Whitney, 1975). Two models were developed to predict this mechanical response of the notched laminate: the Point and Average Stress Criterion (Whitney & Nuismer, Stress fracture criteria for laminated composites containing stress concentrations, 1974). The Point Stress Criterion PSC states that failure occurs when, at a distance of the notch, there is a stress that reaches the strength of the unnotched plate. The Average Stress Criterion ASC states that failure occurs when the average of stresses at a distance from the notch reaches the strength of the unnotched plate. On the other hand, the modified PSC (Pipes, Wetherhold, & Gillespie, 1979), relates the distance at which the stress reaches the strength of the unnotched plate, with

the whole radius, introducing new parameters m and C. A comparison of an example experimental results with the predicted models is analyzed in this Chapter, on [0/±45/0]s and [0/±45/90]s notched laminates.

Specimen preparation

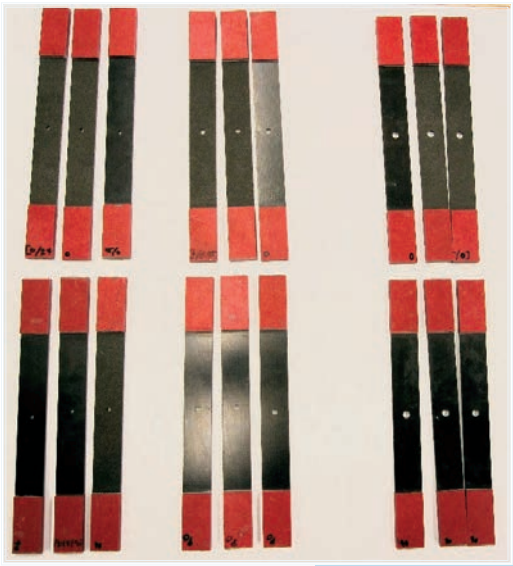

Figure 64. Sample specimens. *Source: Author.*

The particularity of the specimens for this test is basically the whole that they should have in the middle of the specimen. So, depending on the laminate object of study, panels should be manufactured according to the stacking sequenced to be analyzed, as explained in Chapter one, and then, once the panels are cured, wholes should be drilled in the center of the specimen. Whole size depends also on the parameter to be studied. *Figure 63* shows open whole specimens with 3 different whole diameters, which are used as an example during the present chapter. Specimens showed on *Figure 63* are $[0/\pm45/0]_s$ and $[0/\pm45/90]_s$ IM7-8552 Laminate with three different size of holes, as shown in *Table 15*.

Table 15.

Specimen Hole Size

Hole Size	Average hole radius, mm
Small	1.79
Medium	2.53
Large	3.41

Source: Author.

Specimen's average dimensions are shown in *Table 16*.

Table 16.

Specimen average dimensions

Laminate	Avg width, mm	Avg thickness, mm	Avg area, mm^2
$[0/\pm45/0]_s$	25.48	1.38	35.21
$[0/\pm45/90]_s$	25.48	1.39	35.37

Source: Author.

Since the drilling operation may cause fiber tear out due to the pressure applied, holes should be inspected for fiber damage using a microscope.

shows one of the sample specimens inspected with a microscope.

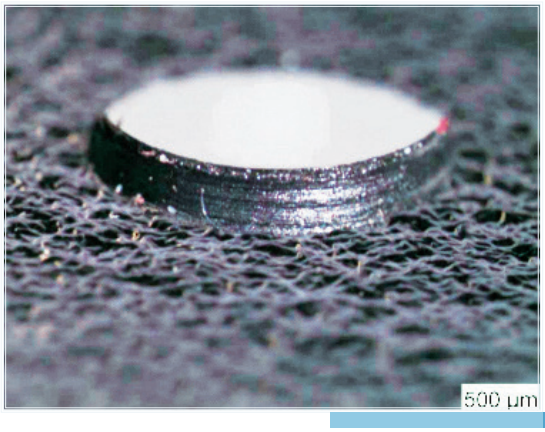

Figure 65. Inspected hole by microscope. *Source: MSE 597 report.*

Materials, tools and equipment

The following materials, tools and equipment are required to an open hole tensile test

- ***Materials***
  - » Specimens
  - » End Tabs
  - » Hysol EA 9394 or other structural adhesive
- ***Tools***
  - » Strain gages (3 x specimen)
  - » Personal protection items
  - » Caliper
  - » Driller
  - » Microscope

- ***Equipment***

  - » Computer
  - » Data acquisition system
  - » Tensile testing machine
  - » Diamond saw or water jet

Procedure

1. The procedure for the open hole tensile test is as follows:
2. Design specimens as explained above
3. Manufacture panels according to Chapter 1.
4. Add the End Tabs
5. Cut panels using a diamond saw or water jet
6. Drilled a hole in the center of the specimen
7. Inspect holes for fiber brakeage with a microscope.
8. Mark each specimen
9. Add transverse and longitudinal strain gages to all the coupons.
10. Measure and register each specimen thickness and width (3 measurements x specimen)
11. Calculate cross sectional area
12. Connect a strain gage (already mounted to the sample) to the data acquisition system
13. Prepare a tensile testing machine displacement controlled and the data acquisition system.
14. Clamp specimen in the tensile tester using the grips, see *Figure 17*.
15. Test specimens at a rate of 1mm/min recording loads and displacements until failure.

Data Reduction

Failure prediction can be done by the Point Stress Criterion PSC, the Average Stress Criterion ASC and the modified PSC proposed by Pipes.

Point Stress Criterion

The open hole test consists on a finite sized plate of with w, with center hole of radius R, subjected to uniaxial tension, as shown in

The ratio of the notched strength to the un-notched strength of an infinite plate can be express by Equation 56.

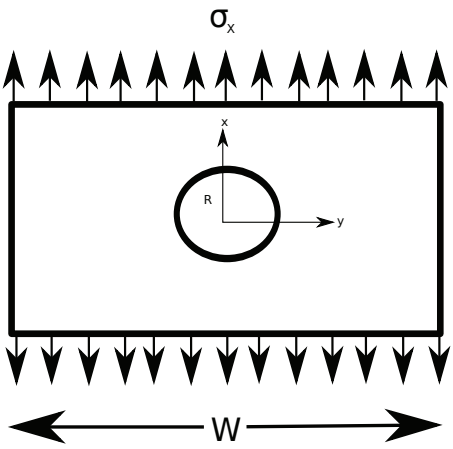

Figure 66. Finite plate with center hole. *Author: MSE 597 report.*

Equation 56

$$\frac{\sigma_N(\infty)}{\sigma_0(\infty)} = \frac{2}{2+\lambda^2+3\lambda^4-(K_\infty-3)(5\lambda^6-7\lambda^8)}$$

Where $\sigma_N(\infty)$ is the ultimate strength of a notched infinite plate, $\sigma_o(\infty)$ is the ultimate strength of an un-notched infinite plate, K_∞ is the stress concentration factor for an infinite plate, and λ is express by *Equation 57*.

Equation 57

$$\lambda = \frac{R}{R + d_0}$$

Where R is the radius of the Hole and d_o is the distance from the hole at which the stress reaches the ultimate stress of the un-notched laminate. The stress concentration factor for an infinite plate K_∞ can be express by *Equation 58*, where the laminate elastic constants can be determined from laminate theory.

Equation 58

$$K_\infty = 1 + \sqrt{2\left(\sqrt{\frac{E_x}{E_y}} - v_{xy} + \frac{E_x}{2G_{xy}}\right)}$$

Average Stress Criterion

Following the ASC, the ratio of the notched strength to the un-notched strength of an infinite plate can be express by *Equation 59*.

Equation 59

$$\frac{\sigma_N}{\sigma_O} = \frac{2}{(1+\delta)\left(2 + \delta^2 + K_\infty - 3\right)\delta^6}$$

Where $\delta = \frac{R}{R + a_o}$

Modified PSC

The modified PSC improve the effectiveness of the PSC by relating the characteristic distance with two introduced parameters c and m, as shown in *Equation 60*.

Equation 60

$$\left(\quad \right)$$

Where m is an exponential parameter, d_o is a reference radius, and c is the notch sensitivity factor.

Aplication of the Criterions

Since the above expressions offer solution for calculating the strength of an infinite plate, and the specimens are obviously finite, then the relation shown in *Equation 61* is used.

Equation 61

$$\sigma_N(\infty) = \frac{\sigma_N(w) K}{K_\infty}$$

Where $\sigma_N(w)$ is the strenght of a finite plate which is determined experimentally, and K is the stress concentration factor for a finite plate. K is determined by *Equation 62*.

Equation 62

$$\frac{K}{K_\infty} = \frac{2 + (1 - D/w)^3}{3(1 - D/w)}$$

Where D is the hole diameter and w is the specimen width. For accuracy D/w should be greater of equal than 4. Then, by calculating K and then substituting to get the strength of the infinite notched plate, one can solve for lambda according to the PSC and the modified PSC, or for delta following the ASC. It is important to notice that the roots of interest are between zero and one.

For the modified PSC one can substitute *Equation 60* in *Equation 57* to get *Equation 63*.

Equation 63

$$\lambda = \frac{1}{1 + R^{m-1} C^{-1}}$$

Having lambda, *Equation 63* can be rearrange to get c and m, by *Equation 64*.

Equation 64

$$-\log\left(\frac{1}{\lambda} - 1\right) = logC + (1 - m)logR$$

Typical experiment results

Specimen used as an example were tested using Sintech 30/D screw driven testing machine rated to $100\,kN$.at a rate of $1mm/min$. Load and displacements were collected in order to identify any abrupt change in the stiffness. The notched laminate strength was calculated. Failure prediction was done using the PSC, ASC and the modified PSC. The laminate elastic constants used in the calculation of the stress intensity are shown in *Table 17*.

Table 17.

Laminate elastic constants

Laminate	Thickness, mm	E_x, GPa	E_y, GPa	ν_{xy}	G_{xy}, GPa
$[0/\pm45/0]_s$	.166	86.03	23.3	0.754	21.91
$[0/\pm45/90]_s$	.166	57.98	57.98	0.322	21.91

Source: Author.

The calculated stress intensity factor for a notched infinite plate and the ultimate stress of the un-notched laminate are shown in *Table 18*.

Table 18.

Stress intensity factor and ultimate stress

Laminate	K_∞	$\acute{o}_0$
$[0/\pm45/0]_s$	3.5	1312
$[0/\pm45/90]_s$	3.0	692.8

Source: Author.

The results from the PSC are plotted and compared with the experimental data in *Figure 67* and *Figure 68* for each laminate. In the same way, the results from the ASC are plotted and compared as well with the experimental data in *Figure 69* and *Figure 70* for each laminate respectively. The predictions match the trend of the experimental data on both cases.

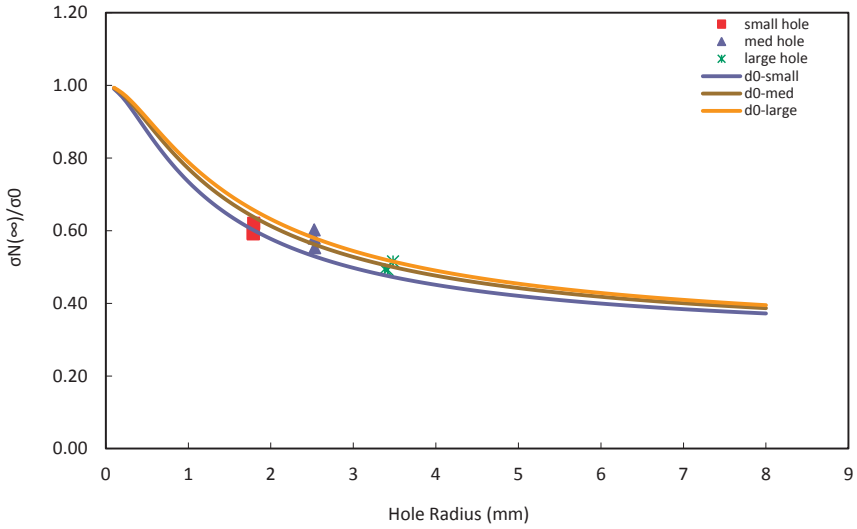

Figure 67. Point Stress Criterion for the $[0/\pm45/0]_s$ *Source: Author.*

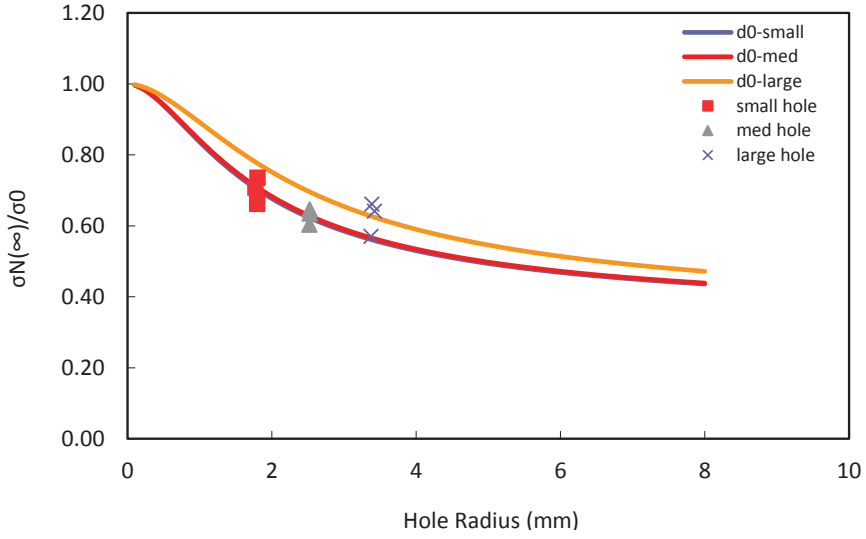

Figure 68. Point Stress Criterion for the $[0/\pm45/90]_s$ *Source: Author.*

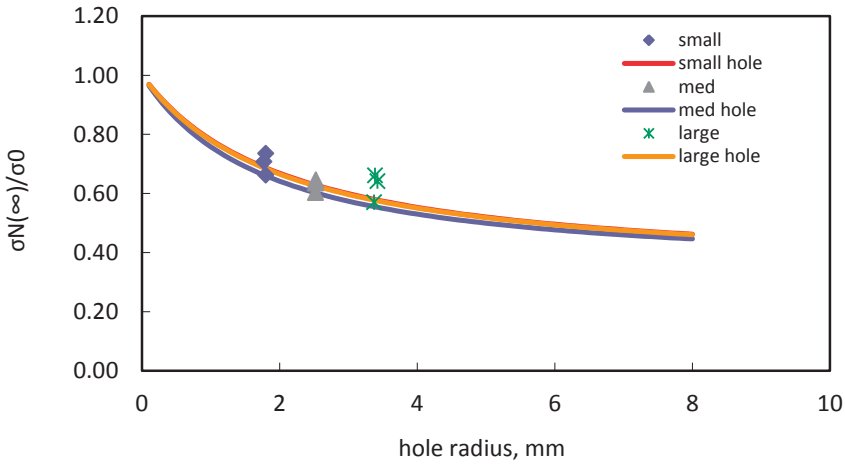

Figure 69. Average Stress Criterion for the $[0/\pm45/0]_s$
Source: Author.

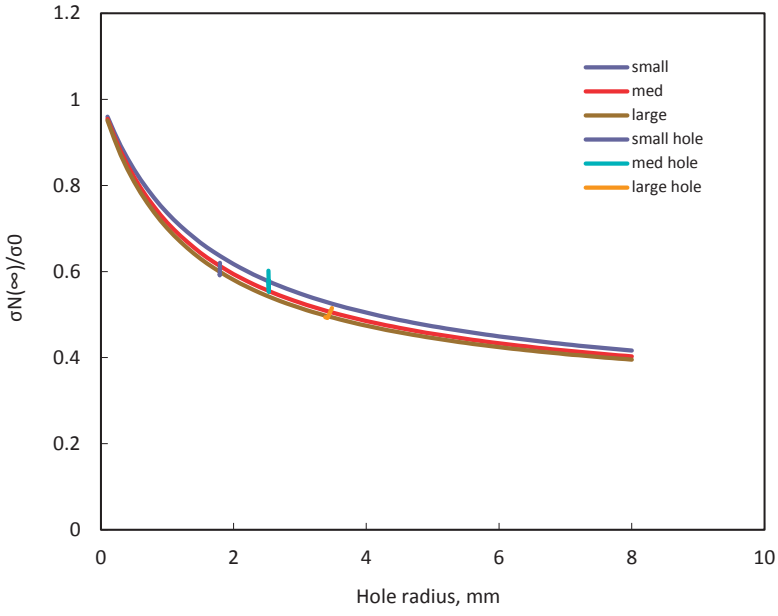

Figure 70. Average Stress Criterion for the $[0/\pm45/90]_s$
Source: Author.

By plotting $-log(1/\lambda-1) vs. log\, R$ as shown in *Figure 71*, the slope and the intercept at $log\, R$ equal to 0 can be obtained by the least squares method. In such a way, the exponential factor m, and the notch sensitivity factor C, are calculated. The results are shown in *Table 19*.

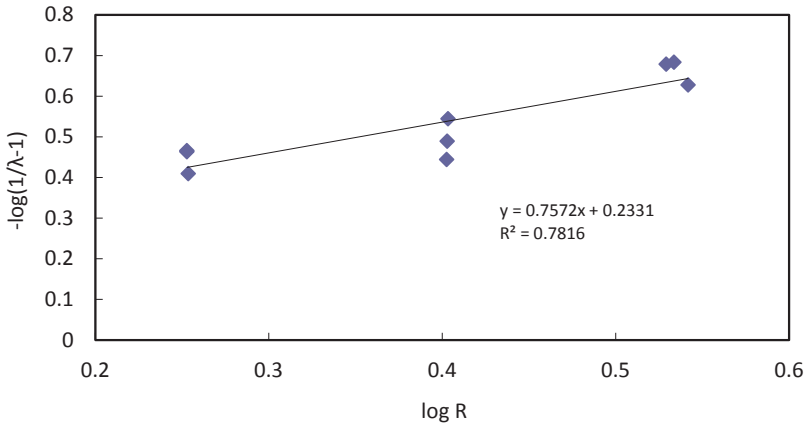

Figure 71. $-log(1/\lambda-1) vs. log R$. *Source: Author.*

Table 19.

Exponential Factor m & Notch sensitivity factor C

Laminate	*m*	C	ã
$[0/\pm45/0]_s$	0.203	1.293	29.38
$[0/\pm45/90]_s$	0.483	1.002	26.15

Source: Author.

For an insensitive material $m=1$ and $C=0$. In order to take a reference point to compare which of the laminates is more sensitive, m is set as $0.1=9$ and C as 0.1. A new parameter is introduced in order to account for the relative notch sensitivity γ. It can be seen in *Table 19*, that the $[0/\pm45/0]_s$ laminate is more sensitive that $[0/\pm45/90]_s$

. This phenomenon has a correlation with the number of zero degrees plies in the laminate, which make the laminate more sensitive.

The Notch sensitivity of the $[0/\pm45/0]_s$ and $[0/\pm45/90]_s$ laminates is shown in *Figure 72*. The upper bound is related to the reference parameter $m*C*$ and the lower bond is $1/k_\infty$. The experimental data has the same trend as the predicted theoretical for both laminates. When the radius of the hole increases the theoretical curves approaches the value of $1/k_\infty$ in each case.

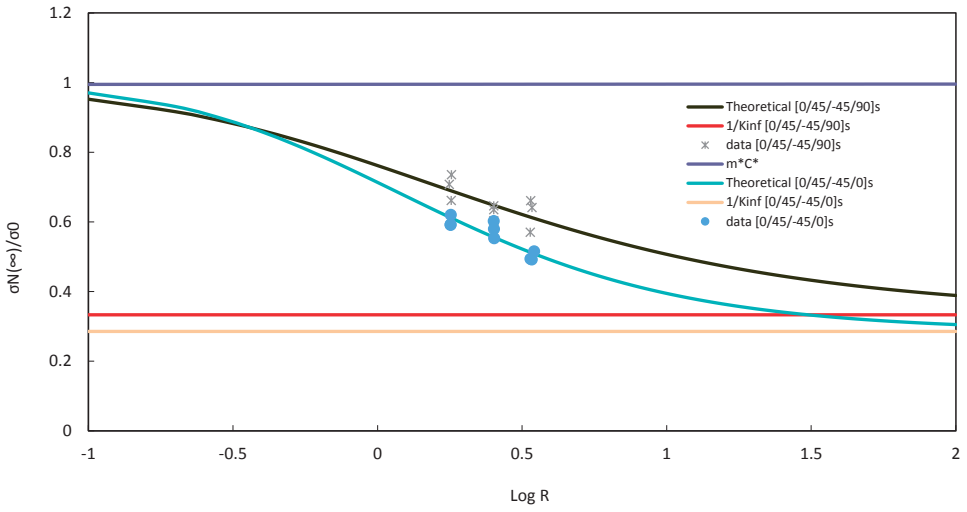

Figure 72. Notch sensitivity of $[0/\pm45/0]_s$ & $[0/\pm45/90]_s$ laminates. *Source: Author.*

The failure of notched specimens is complex. It involves delamination, pull out of the fibers and matrix cracking. The hole acts as a free edge, so the free edge effect is produced. As a result, failure is dominated by delamination and it increases with the hole size. *Figure 73* and *Figure 74* show the delamination on a failed specimen. The fracture zone is a region close to the notch, so if the hole is small comparing with the width and length of a specimen, the material acts as if there were no hole at all.

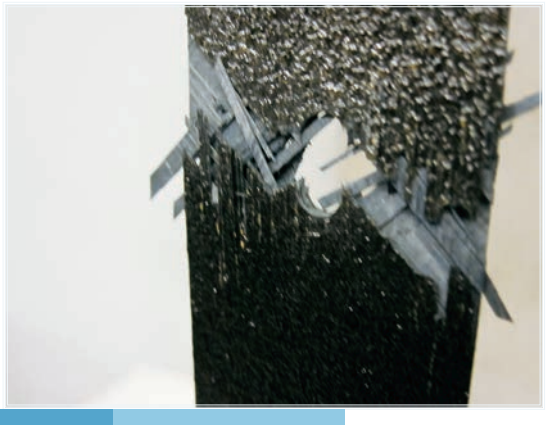

Figure 73. Failed specimen. *Source: Author.*

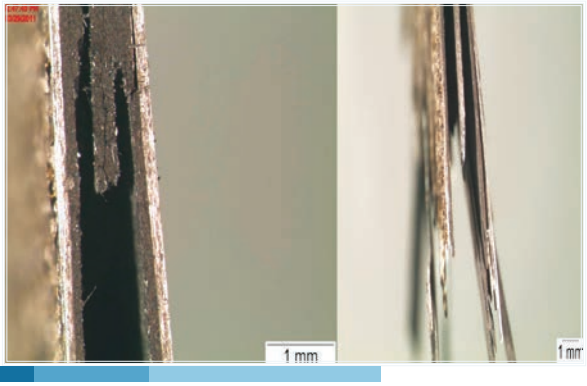

Figure 74. Photomicrograph of the failed specimen. *Source: MSE 597 report.*

Conclusions

All laminates failed at the hole and not the grips. Delamination was the dominated mode of failure, and besides, holes act as free edges. The tensile strength of composite laminate with a circular hole is a function of the size of the hole. The strength of the laminate is inversely proportional to the hole size. The modified PSC method give a better idea of overall how sensitive the laminate is to different hole sizes. Modified PSC provides one number γ for comparison of notch sensitivity. The notch sensitivity in the laminate increases with the number of zero degree plies. If the hole is small in comparison to the width and length, the strength of the laminate could be the un-notched strength.

References

Cruse, T. A. (1973). Tensile strength of notched composites. *Journal of Composite Materials,* 7(2), 218-229.

Nuismer, R. J., & Whitney, J. M. (1975). Uniaxial failure of composite laminates containing stress concentrations. *Fracture mechanics of composites, ASTM STP, 593,* 117-142.

Pipes, R. B., Wetherhold, R. C., & Gillespie, J. W. (1979). Notched strength of composite materials. *Journal of Composite Materials,* 13(2), 148-160.

Whitney, J. M., & Nuismer, R. J. (1974). Stress fracture criteria for laminated composites containing stress concentrations. *Journal of Composite Materials,* 8(3), 253-265.

Chapter 9

Characterization of Delamination Failure: Mode I Fracture

Chapter 9

Characterization of Delamination Failure: Mode I Fracture

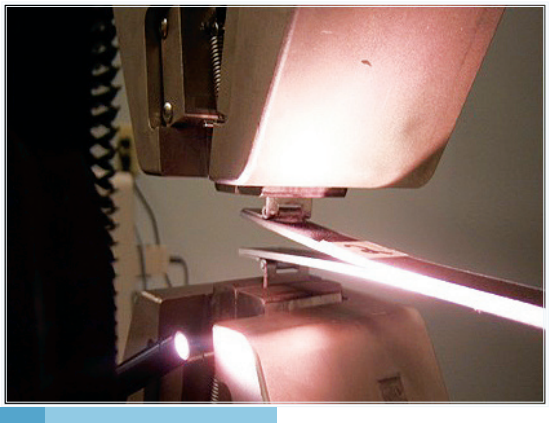

Figure 75. Mode I Fracture Test. *Source: MSE 597 report.*

Delamination failure has been one of the dominant types of failure in composite materials (Robinson, 1987). Delamination can be induced by defects during the layup or may appear during loading service of the material cause by the free edge effect. The delamination process has been represented as the growth of a crack like discontinuity (Wang, 1983). As a result, it is convenient to analyze it by fracture mechanics.

There are basically two approaches in fracture mechanics for finding the fracture toughness of a crack material: Stress intensity Factor and Energy release rate. Since the idea is to do experimental characterization, the energy release approach is more appropriate. In this, the fracture toughness is the work done to generate a new crack. However, it is important to point out that the fracture mechanics analysis of delamination in composites is only appropriate for the analysis of unidirectional zero degrees laminates. The Double Cantilever Beam specimen is used for the analysis of delamination process by Mode I of fracture (ASTM D5528, 2013).

As an example, during the current Chapter it will be discussed a test was conducted according to the ASTM Standard D 5528 on $[0]_{24}$ DCB specimens. They were tested in Mode I fracture loading conditions, measurements of the crack generated were taken. A correction factor in the compliance calculation was applied. The work done by each crack extension was calculated as the energy release rate.

Specimen Preparation

Specimens should be design according to ASTM Standard D 5528. An example is shown during the chapter for a $[0]_{24}$ carbon epoxy laminate manufactured by *prepreg* lay-up and cured in autoclave. A $0.002\,mm$ thick Teflon sheet was placed in the laminated middle plane in order to induce a crack. Specimens were cut from the laminate as shown in *Figure 76*.

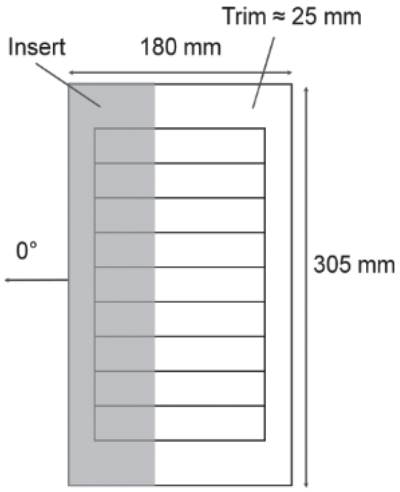

Figure 76. Specimen's manufacturing sketch. *Source: Author.*

Piano hinges were bounded to the specimens in the induce crack side with structural adhesive as shown in *Figure 77*. Specimen's dimensions and induced crack length are shown in *Table 20.*

Figure 77. Mode I fracture specimens.
Source: Author.

Table 20.
Specimen's dimensions

Sample	Insert Length a_0, mm	Avg width, mm	Avg thickness, mm
S1	64,37	25,45	4,09
S2	64,03	25,53	4,13
S3	65,17	25,47	4,10
S4	64,86	25,38	4,08
S5	62,8	25,54	4,03
Total average		24,53	4,06
Total SD		1,73	0,05

Source: Author.

Materials, tools and equipment

The following materials, tools and equipment are required for Characterization of Delamination Failure-Mode I Fracture of composites:

- ***Materials***
  - » Specimens
  - » Hinges
  - » Hysol EA 9394 or structural adhesive

- ***Tools***

  - » Strain gages (1 x specimen)
  - » Personal protection items
  - » Caliper

- ***Equipment***

  - » Computer
  - » Stereoscope
  - » Data acquisition system
  - » Tensile testing machine with fixture with 2 point supports as shown in *Figure 39*.
  - » Diamond saw or water jet

Procedure

1. The procedure to perform characterization of Delamination Failure-Mode I is the following:
2. Design specimens according to ASTM Standard D 5528.
3. Manufacture panels according to Chapter 1.
4. Cut panels using a diamond saw or water jet.
5. Add piano hinges with structural adhesive.
6. Depending on the material color, painting of the transverse area where crack propagation is visible may be required, since every crack propagation should be mark with a pen.
7. Mark each specimen.
8. Measure and register each specimen thickness and width (3 measurements x specimen).
9. Prepare the set up with a testing machine displacement controlled, a stereoscope and the data acquisition system as shown in *Figure Figure* **78**.
10. Put the specimen on the testing area.
11. Grip the piano hinges with the tensile testing machine.

12. Verify and adjust the stereoscope so that it captures the transverse specimen area where crack is going to propagate. Recommended magnification $10X$
13. Start the test loading the specimens at a rate of $2mm/min$ recording loads and displacements, and paying close attention to the load displacement curve. Stop the machine when detecting load drops.
14. Mark with a pen the crack tip.
15. Take a picture of the crack.
16. Measure crack length using image processing software.
17. Unload the tensile testing machine.
18. Repeat steps 12 to 13 until crack propagates through the whole specimen.

Figure 78. Testing equipment. *Source: MSE 597 report.*

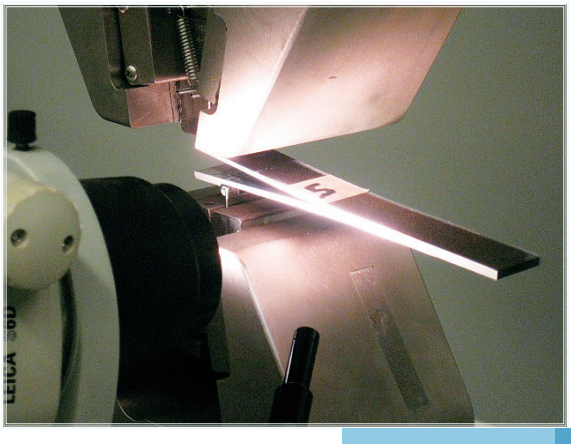

Figure 79. Specimen during the test.
Source: Author.

Data Reduction

The strain energy release rate for a structure tested in Mode I fracture is given by *Equation 65*, Where P is the applied load, is the width of the structure, and $\frac{dC}{da}$ is the change in compliance of the structure with a variation in crack length.

Equation 65

$$G = \frac{P^2}{2\mathrm{w}} \frac{dC}{da}$$

The specimen is assumed to be a Double Cantilever Beam with each beam rigidly attached into the specimen, so that beam theory can be applied to calculate the compliance. However, it is know that the assumption is not correct taking into account the finite size of specimen and the high stress presented at the crack tip. Berry proposed a relation of the compliance with a power crack length shown in *Equation 66*, to correct the effect of the assumptions made. In *Equation 66*, a is the crack length and H and n are parameters determined from the crack extension, load and displacement data.

Equation 66

$$C = \frac{a^n}{H}$$

If the stiffness of the specimen at the point of crack growth (P_c / δ_c) is plotted versus the crack length a in a doble logarithmic graph, then, n is the slope of the best fit line applied to the data. P_c and δ_c are the critical load and displacement associated with each crack length. Then, the energy release rate can be express as *Equation 67*.

Equation 67

$$G_{Ic} = \frac{nP_c\delta_c}{2\text{wa}}$$

Since the energy release rate expressed in *Equation 67* is calculated for each crack extension, the energy release rate of the specimen is the average of those values.

Typical Load Displacement Behavior

Typical behavior during a Mode I Fracture test is explained using the example of three specimens tested in tension using a Sintech 30/D screw driven testing machine $100\,kN$ rated to which piano hinges were gripped, and then tension was applied at a rate of $2mm/min$. The machine was stopped when a drop in the load displacement curve was presented. A pen was used to mark the crack tip of each event; should clarify that the measurements of the crack extension were taken using image processing software. An example of an image taken is shown in *Figure 80*. Specimens were unloaded and a new loading cycle was done recording the same information for each cycle, until crack propagation was unstable.

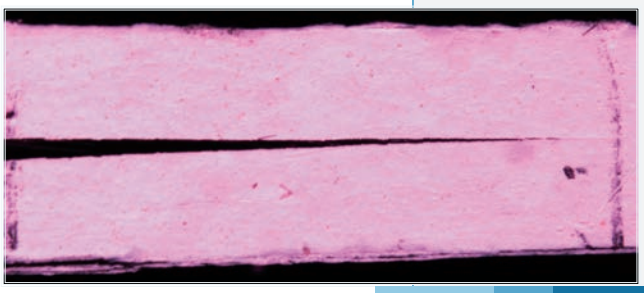

Figure 80. Crack extension. *Source: MSE 597 report.*

A typical load displacement behavior is shown in *Figure 81*. It is the representation of an experiment used as example for the Chapter. The behavior is as expected with respect to the theoretical. It can be seen that the critical load for the first case is higher than the rest. This is due to the fact that the induced crack is not as sharp as the other ones. In turn, and because of that, the behavior is affected and Linear Elastic Fracture Mechanics should not be applied for the first data.

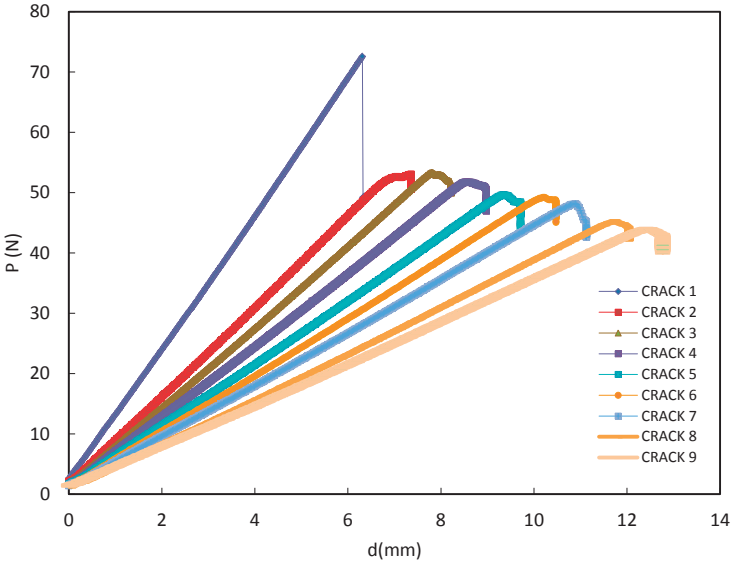

Figure 81. Load versus displacement graph. *Source: Author.*

Data reduction

Crack extension measurements for each specimen are shown in *Table 21*.

Table 21.

Crack extension measurements for each specimen

Crack length a_i, mm	Specimen			
	2	3	4	5
a_0	64,03	65,17	64,86	62,8
a_1	72,84	67,41	69,1	65,47
a_2	77,79	76,97	74,61	69,39
a_3	81,83	87,35	79,22	74,88
a_4	84,51	96,07	83,47	79,14
a_5	87,94	105,51	87,74	84,39
a_6	91,43		92,12	
a_7	94,23			
a_8	98,07			

Source: Author.

Figure 82 and *Figure 83* show the result of the calculation of the n parameter by plotting the inverse of the compliance versus the crack length in a double logarithmic graph.

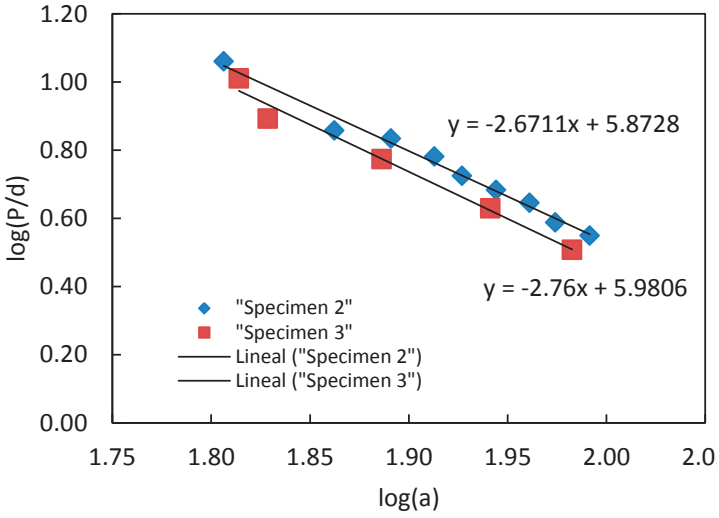

Figure 82.
Determination of parameter *n* for specimens 2 and 3.
Source: Author.

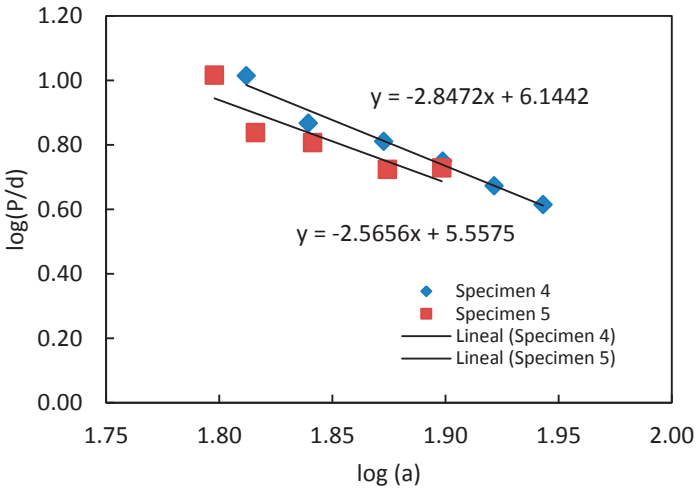

Figure 83. Determination of parameter *n* for specimens 4 and 5. *Source: Author.*

The plot of the energy release rate versus the crack length is shown in *Figure 84*. It is important to notice that the first crack extension is not taken into account in the calculation since the induce crack is not sharp, so the linear elastic fracture mechanics does not apply in that case. The total energy release rate is the average value of each specimen energy release rate obtained by the linear curve fit shown in *Figure 84*. Results are shown in *Table 22*.

Table 22.

Energy release rate

Specimen	$G_{IC}(J/m^2)$
2	228.81
3	260.74
4	213.24
5	281.14
Average	245.98
S.D	30.66

Source: Author.

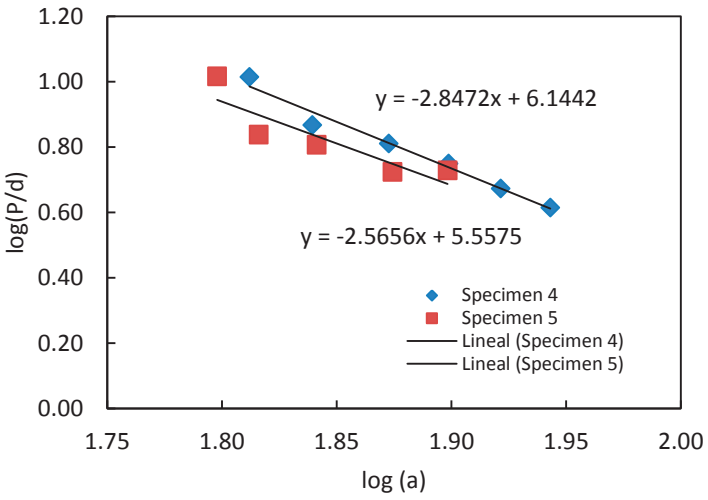

Figure 84. Energy release rate versus crack length. *Source: Author.*

Conclusions

Daniel's book on composite materials gives a range of values for GIC between $80 J/m^2$ and $250 J/m^2$ for various carbon/epoxy composite materials. According to the experimental results used as example during the chapter, the maximum energy release rate is approximately $25\ J/m^2$ and the minimum is $25\ J/m^2$ approximately. The minimum value is within the range while the maximum value is a little bit out of the normal range. However, it is reasonable taking into account the number of specimens tested and the equipment and process used to measure the crack extension which can induce some error. It could be seen during the experiment that the stiffness of the specimens decreases as the crack propagates. As a result, the compliance of the specimen's increases as the crack propagates through the specimen.

The initial blunt crack increases the fracture toughness; that is the reason for the sudden drop in the initial crack. Besides, since the induced crack is not sharp, linear elastic fracture mechanics does not apply in that region. As a result, the

first data should not be considered in the calculations. Also, the fiber bridging effect is still present and tends to increase the fracture toughness

References

ASTM D5528. (2013). *Standard Test Method for Mode I Interlaminar Fracture Toughness of Unidirectional Fiber-Reinforced Polymer Matrix Composites.* West Conshohocken, PA: American Society for Testing and Materials.

Robinson, D. A. (1987). Failure M[illegible]s in Composite Materials. *NAVAL ACADEMY ANNAPOLIS, USNA-TSPR*-148.

Wang, S. S. (1983). Fracture mechanics for delamination problems in composite materials. *Journal of Composite Materials,* 17(3), 210-223.

Por favor cambia a minúscula solo dejar las primera en mayúsculas
Naval Academy Annapolis (en cursiva) Gracias.

Graduate School of the
Colombian Air Force

Science and Air Power Collection

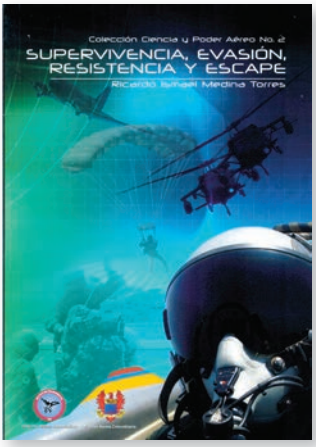

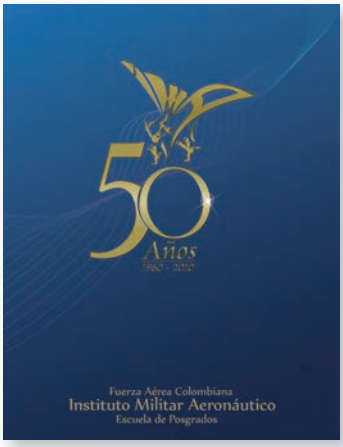

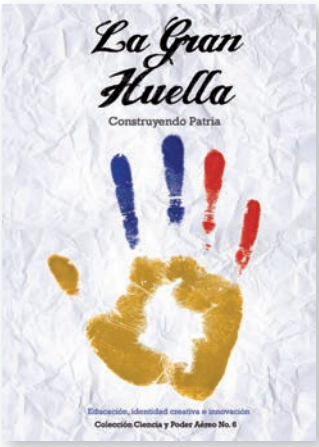

Carrera 11 No. 102-50 Building ESDEGUE, office 411
Bogota, Colombia. A.A. 110111
Tel: (0571) 6378927 - (0571) 6206518 Ext. 1700

About the author

Lieutenant Peter Rolando Alvarado Prieto is the Lead Engineer of the Calima T-90 aircraft project at the Colombian Air Force, and is also the principal researcher of a project on Fatigue Analysis of adhesive Joints. He holds a Master's degree in Aerospace Engineering from Purdue University and a Bachelor of Science in Mechanical Engineering from the Colombian Air Force Academy. He has worked in the past as a structures engineer and researcher, where he has gained hands on knowledge on composite materials and characterization of advanced composites. He has experience in design, manufacturing, testing, and characterization of composites. Mr. Alvarado has received several distinctions during his military career for his outstanding performance: he graduated with honors from the Air Force Academy, received medals from the Korean Republic, Chile, and Italy, and honorary pilot wings from Brazil and Peru. He was also awarded with one of the most prestigious scholarships, Fulbright-COLCIENCIAS-DNP scholarship. Lieutenant Alvarado is an active member of the Colombian Air Force Graduate School research group and was a member of the Air Force Research Center on Aerospace Technology where he participated in several projects.